

2
E. Adil
15/11/1541

**Integrated Reservoir Characterization of Miano Area,
Lower Indus Basin, Using 2D Seismic and Well Log Data**



By

Muhammad Asif

MSc. (GEOPHYSICS)

DEPARTMENT OF EARTH SCIENCES

QUAID-I-AZAM UNIVERSITY

ISLAMABAD

2014-2016

CERTIFICATE

This dissertation, submitted by **Muhammad Asif** is accepted in its present form by the Department of Earth Sciences, Quaid-i-Azam University Islamabad as satisfying the requirement for the award of MSc degree in Geophysics.

RECOMMENDED BY

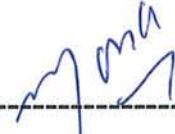
Dr. Aamir Ali

(Supervisor)



Dr. Mona Lisa

(Chairperson Department of Earth Sciences)



External Examiner

**DEPARTMENT OF EARTH SCIENCES QUAID-I-AZAM
UNIVERSITY ISLAMABAD,**

2014-2016

ACKNOWLEDGEMENT

All the praise and appreciations are for the creator of the whole universe to God, who knows better the mysteries and secrets of the universe and shares it with us by blessing sense and thirst for knowledge. It is all due to HIS guidance that we know about the subsurface, space and little about our universe.

I am especially indebted to my thesis supervisor **Dr. Aamir Ali** for giving me an initiative to this study. His inspiring guidance, dynamic supervision and constructive criticism enabled me to complete this thesis work. I am greatly honored to pay my deeply gratitude to whole faculty of my department especially **all the teachers** whose valuable knowledge, assistance, cooperation and guidance enabled me to take initiative, develop and furnish my academic carrier and pay humble regards to **Dr. Mona Lisa (Chairperson Department of Earth Sciences)** for her cooperation.

I feel pleasure and honor to express my thanks to my senior Muhammad Kashif , Ashar jadoon and Zahid -u- llah khan friends ,Farhan , Liquit Ali ,Muhammad kamran, Muhammad Saim Zafer, and Raja Fahad for their great support, encouragement and friendly attitude during the present study and throughout the period of MSc.

Finally, I owe all my academic success and progress in life to my loving parents and sisters, and brothers, and cousin whose affection, endless prayers, good wishes and inspiration remained with me for higher ideals of life.

Muhammad Asif

TABLE OF CONTECTS

CHAPTER-01

INTRODUCTION

1.1 Introduction.....	1
1.2 Introduction to Miano Area.....	2
1.3 Previous Work in the Project Area.....	2
1.4 Data Set Used.....	3
1.5 Aims and Objective.....	4
1.6 Methodology.....	4
1.7 Significance.....	6

CHAPTER-02

GEOLOGY

2.1 Introduction.....	7
2.2 Geologic and Geographic Location of Study Area.....	7
2.3 Structural setting of Southern Indus Basin.....	8
2.4 Stratigraphy of the Study Area.....	8
2.5 Petroleum System of Study Area.....	8

CHAPTER-03

SEISMIC INTERPRETATION

3.1 Introduction of 2D seismic Data.....	13
3.2 Basic Workflow of Seismic Interpretation.....	13
3.3 Seismic Tie	17
3.4 Seismic Interpretation.....	17
3.5 Time Contour Maps.....	22
3.6 Velocity Analysis.....	22
3.6 Depth Contour Maps.....	23
3.7 3D view of Fault Polygon.....	23
3.8 Generation of Synthetic Seismogram.....	24

3.9 Seismic Attributes.....	32
-----------------------------	----

CHAPTER-04 PETROPHYSICS AND FACIES ANALYSIS

4.1 Introduction.....	37
4.2 Classification of Geophysical log.....	37
4.3 Average Porosity Calculation.....	40
4.4 Effective Porosity.....	41
4.5 Mathemsticsl relation for water Saturation.....	41
4.6 Interpretation of Well Log.....	42
4.7 Rock Physical Relation.....	43
4.8 Facies Analysis.....	44

CHAPTER-05 ROCK PHYSICS

5.1 Introduction to Rock Physics.....	47
5.2 Rock Physical Analysis.....	47
5.3 P-Wave (Primary wave)	48
5.4 S-Wave (Secondary wave).....	48
5.5 Poisson Ratio.....	49
5.6 The V_p , V_s Ratio	50
5.7 Velocity Relation With depth.....	50
5.8 Yonug's Modulus	51
5.9 Bulk Modulus	52
5.10 Shear Modulus	52

CHAPTER-06 SEQUENCE STRATIGRAPHY

6.1 Overview.....	53
6.2 Sequence Stratigraphy.....	53
6.3 Sequence.....	53
6.4 Sequence Stratigraphy and Sea Level Change.....	53
6.5 Depositional Environment Related to Well log.....	55
6.6 C-interval.....	55
6.7 B-interval.....	55

CHAPTER-07 AMPLITUDE VESUS OFFSET (AVO)

7.1 Introduction.....	58
7.2 Amplitude versus Offset (AVO) Analysis.....	58
7.3 Zoeppritz equation.....	60
7.4 Shuey Approximation.....	60
7.5 Rouger Approximation.....	61
7.6 AVO Classification.....	61
7.7 AVO analysis in the Study Area.....	63
7.8 Wavelet analysis.....	64
7.9 Convolution Ricker Wavelet with Exact, Shuey and Rouger.....	66
7.10 Velocity and Lithology.....	67

Abstract

In hydrocarbon exploration the seismic method is the most modern technique being used by the petroleum industries. It is the most accurate and gives detailed information about the subsurface as compared to other available geophysical methods. But due to anisotropic behavior and structural complexities the risk also prevails there. This may lead to predict the subsurface picture wrongly and as a consequence well failure may occur. This dissertation debates on the possible well failure causes in the Punjab platform area. The 2D seismic data of the study area was used to study the possible well failure cause in the study area.

The present study focuses to understand the possible clue about the reservoir using seismic, well log data and also doing AVO analysis. Seismic data was used understand the subsurface structures of the study. The petrophysical analysis in addition, helped to study the reservoir characterization. Furthermore the depth of different reflectors was calculated by using seismic velocities to calculate the percentage error in depth calculation.

Seismic attributes analysis of seismic section helps in identifying the different lithological boundaries and also the structural disturbance. Different seismic attributes (Signal Envelope, Instantaneous Phase and Instantaneous Frequency) were derived in the study and these attribute confirm about all the interpretation.

Rock physics have been done to understand the reservoir characteristics and to protect from the well frailer. These properties is calculated from the sonic log are used for purposes.

Sequence stratigraphy has been done with the help of GR log. Through this study there is defined the depositional environment of the area is interpreted.

Amplitude versus offset (AVO) analysis is basically used to understand the class of sand in the reservoir.

1.1 Introduction

The seismic method is used in exploration in 1915s and this will give information about imaging about the subsurface geological structure and this will help us to get information about the change in behavior of the subsurface, Chopra & Marfurt, (2005). The seismic refraction method is failed to find out the anomalous zone that's why reflection method is used. After that the reflection method is become the most important method in finding the anomalous zone in the oil and gas industries.

Rock physics is a tool which is helpful in determining the physical properties of rocks in the real earth velocity varies laterally as well as vertically. These properties will effect that how seismic wave physically behave through the subsurface material. Relations between physical rock properties and seismic behavior therefore require

- Knowledge about seismic behavior and physical properties of rock's pore fluid and rock frame.
- Models for rock-fluid interactions (Dewar, 2001).

Amplitude versus offset analysis is applied on the seismic data to find out the fluid content present in the rock, density, porosity and the shear wave information. This will depend on the reflection coefficient and the angle of incident relationship.

In AVO, the offset is varies in order to change the angle of incidence (Katchmart et al., 2010).

For the hydrocarbon investigation Seismic reflection method plays a vital role. By 3D survey of seismic data over a field, that is producing and being developed at proper interval of time, we interpret the variations in the reservoir environments such as pore pressure and fluid saturation (Yilmaz, 2001).

Faults being helpful in describing the geology of the area while Mapping is done often for reflections and Faults also helpful in finding out the hydrocarbon potential zone (Badely, 1985).

Reservoir description can be done by the borehole data as it play important role. Petrophysical analysis such that porosities measurements, water saturation, fluid contacts, volume of shale and reservoir zonation have a great concern (Fischetti et al., 2002)

For improving the subsurface image Forward modeling has been used (Fagin, 1991). The Structural interpretation is the most common application of the forward modeling, (Mellman & Kunzinger, 1992).

1.2 Introduction to Miano Area

Lower Indus Basin comprises of the southern part of the largest Oil & Gas producing Indus Basin and covers the south eastern part of Pakistan. Miano area lies 62km southwest of the Sukkur. In the Miano area eight wells have been drilled in the Lower Goru Formation. Latitude and longitude of upper left 27° 36' 35.9" and 69° 12' 57.1", upper right 27° 36' 35.9" and 69° 27' 30.4" lower left 27° 14' 18.4" and 69° 12' 43.1" and lower right 27° 14' 10.1" and 69° 27' 51.8". Map of the study area is shown in Figure 1.1.



Figure 1.1: Location map of the study area (www.google-earth.com).

1.3 Previous work in the Project area

Eni (formerly known as LASMO Oil plc. of U.K.) discovered a large amount of gas reserve in 1989 in Sandstone of Lower Goru (Cretaceous age) in Lower Indus Basin. This

discovery involved the concentration of many E & P companies for the exploration of hydrocarbon from Lower Goru Sandstone. Since that time many discoveries have been made that are listed below;

- Sawan and Miano Gas Field by OMV
- Mari Deep Oil & Gas Field by Mari Petroleum Gas Company Ltd (MPGCL)
- Rehmat Oil & Gas Field by Petronas (Memon, 2010).

1.4 Data set used

The Seismic data and well data are provided by Directorate General of Petroleum Concessions, Pakistan and Land Mark Resources (LMKR), Islamabad, Pakistan. The available seismic and well data has been loaded in Kingdom (HIS) and the base map is obtained which shows the seismic lines and well location. One well is used to study the area which is miano-09. Details of seismic and well data are given in the Table 1.1& 1.2.

Table 1.1: Detail of Seismic 2D Lines.

Seismic Lines	Shot point	Length(km)	Acquired
GP2094-213	101-738	32	OMV
GP2094-215	101-850	37.621	OMV
GP2094-217	101-915	40.795	OMV
GP2094-219	101-1140.5	52.433	OMV
GP2094-221	101-1141	52.314	OMV
GP2094-223	101-1152	52.780	OMV
GP2094-214	101-1177	53.837	OMV
GP2094-216	101-1035	47.025	OMV

Table 1.2: Detail of Well Data.

Well Name	Well Depth	Formation Top(Lower Goru)	X-axis and Y-axis	Status
Miano-09	3385	2261	527064.55 13041610.57	Development Gas

1.5 Aims and Objectives

- For structural and stratigraphic interpretation, all the available geological and geophysical data (Seismic and Well data) have been utilized.
- Seismic interpretation has been performed to find the possible reservoir characteristic and estimate the extents of reservoir in the area.
- Petrophysical analysis has been performed using well data to find out the capability of storing and transmitting hydrocarbons.
- Facies modeled has been performed using well data to identify various geological units at the reservoir level encountered in the study area.
- Rock physics will be performed to find out the rock characterization.
- Stratigraphy is used to find out the depositional environment.
- AVO analysis is done to classify the class of sand.

1.6 Methodology:

- Review the existing literature to completely understand the geology, stratigraphic and tectonic set-up of the study area.
- 2D Seismic interpretation is performed using commercial software, mainly named as IHS Kingdom software.
- Using the interactive tools of IHS Kingdom software for applying seismic attributes.
- To compute petrophysical properties of reservoir, well logs data are used.
- Amplitude versus offset (AVO) and the rock physical analysis are computed by using the reservoir well logs data are used.
- For the future prospects, possible recommendations on the basis of final results.

Methodology adopted to achieve the desired goals by this research work is illustrated in Figure 1.2.

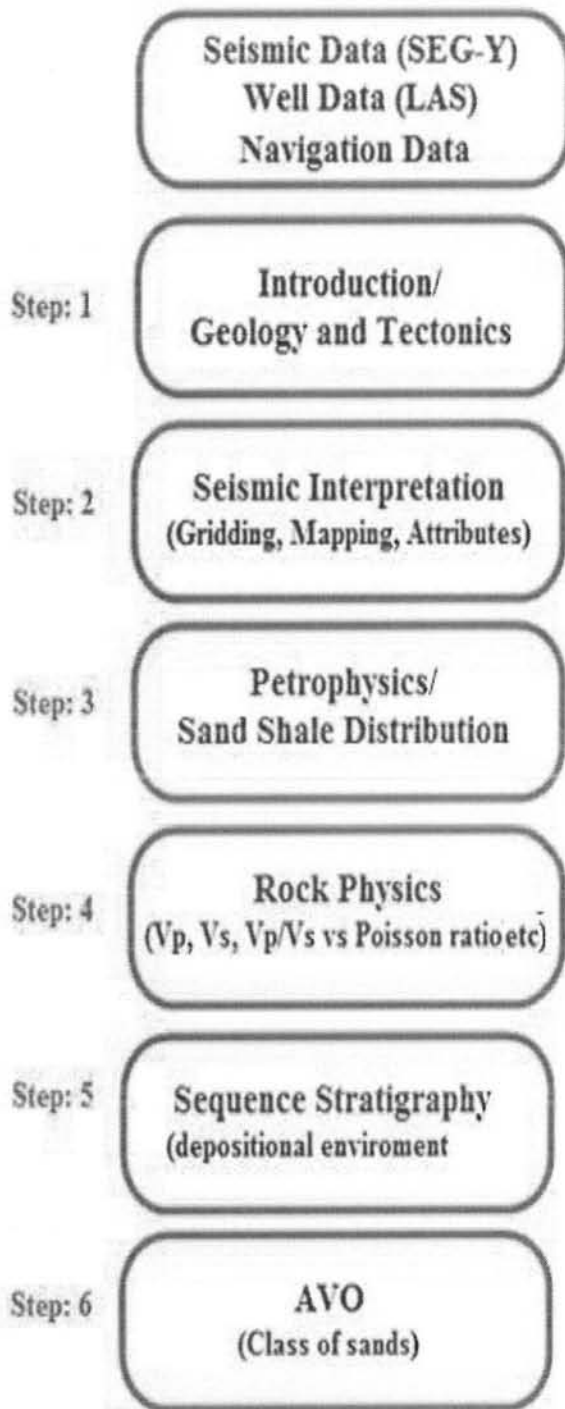


Figure 1.2: Scheme of thesis

1.7 Significance

This research work will be helpful for identification of subsurface structures Miano area that is favorable for hydrocarbon accumulation and trapping. Seismic attribute application on 2D seismic data will prove helpful for confirmation of structural interpretation and potential at the reservoir levels. Facies modeling gives information about the lithology's properties while Petrophysics analysis that is done with help of the well data, gives information about the reservoir in the required area of interest. By integrating all these geophysical techniques possible hydrocarbons zones can be identified and new potential zones can be marked.

2.1 Introduction

Geological history and the geology of the area play important role in the exploration of hydrocarbon. Tectonics and the depositional sequence have their significance role in collecting the information about the basin (Kazmi and Jan, 1997). For the interpretation of the seismic data, geology of the area play its vital role and without having precise information about the geology; we are unable to pick the different horizons in the seismic data. For structural analysis (faulting and folding) in the area is determined by the tectonic history of the area. The area of study is located in lower Indus basin extended approximately between latitude 24° to 28° N and 66° to 68° E (eastern boundary of Pakistan).

2.2 Geologic and Geographic Location of Study Area

The area of study is situated in Lower Indus Basin. The boundaries of the Lower Indus Basin are given in the Figure 2.1. Geogaphic boundaries of the study area is given in Figure 2.2

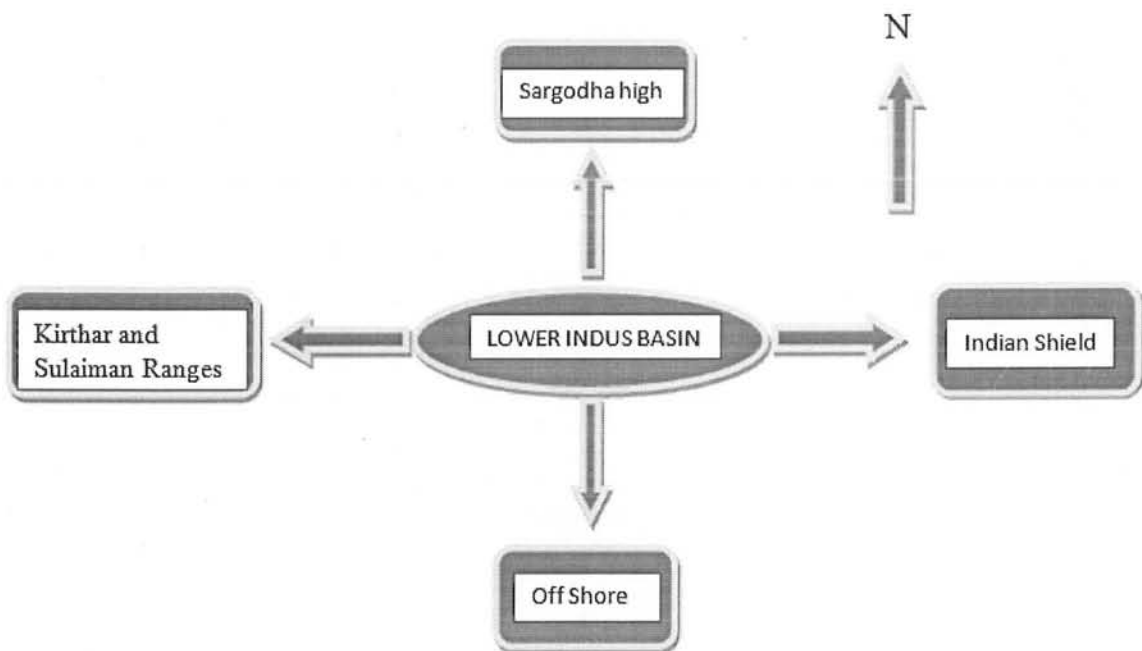


Figure 2.1: Boundaries for the Lower Indus basin.

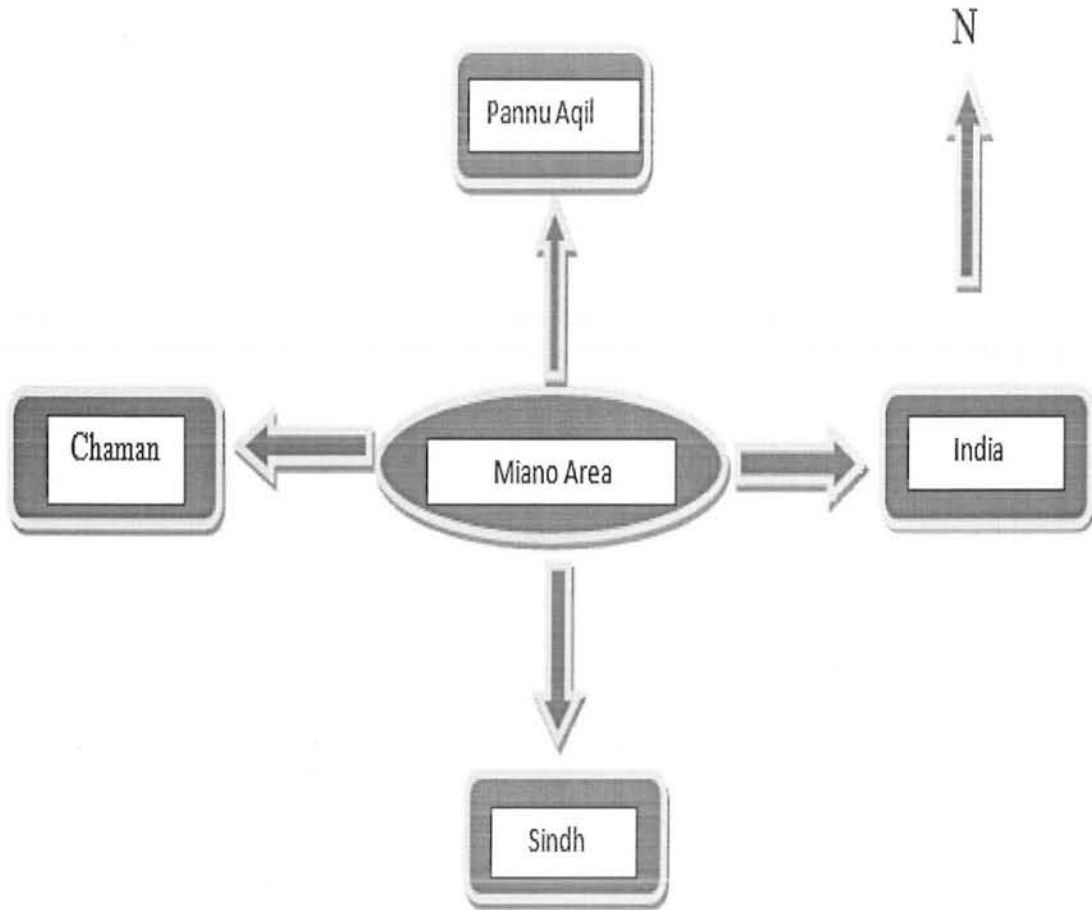


Figure 2.2 Geographic Boundaries of Miano area

2.3 Stratigraphy of the Study Area

The stratigraphy of the area is critical in prospective of the hydrocarbon. Through this knowledge, the information about the reservoir rock is determined. Miano area consists of Eocene age rock to the Cretaceous age rock. The total thickness of the sedimentary basin is few thousands kilometer. Most of these rocks are deposited in shallow marine condition. Study area's stratigraphy is given below in Figure 2.3.

2.4 Petroleum System of the Study Area

In geology, a petroleum play is very important part for the oil and gas Exploration Company's. It will contain the mature source rock and reservoir rock, trap and seal appropriate relative timing of formation. The most important in the petroleum play is the time, upon which the hydrocarbon is reached into its maturation stage (Stoneley, 1995).

Lower Indus basin is producing the 37% hydrocarbons in Pakistan. This main production for the hydrocarbon is obtained from the Lower Indus Basin, Kadri (1995). Source rock, reservoir rock and seal rock is shows in the stratigraphic column of the area.

2.4.1 Source Rocks

In Lower Indus Basin, shale of the sembar formation that is cretaceous age proves to be the source of oil and gas. The Goru formation is rich in hydrocarbons.

2.5.2 Reservoir Rock

Primary objective in this area is the basal sand of the Lower Goru (Cretaceous) formation. Such kind of the sand becomes a source of production in Miano-09, Miano-10, jakhro, bobli and kadanwari fields. Average porosities for such sand are around about 11% in the prospect area.

2.5.3 Seal Rock

The C-interval in the Lower Goru is directly overlying on the Sawan reservoir sand. Thick shales and marls are of the Lower Goru Member from the regional top seal. Shale and tight sands act as the lateral and bottom seals within the "C" interval.

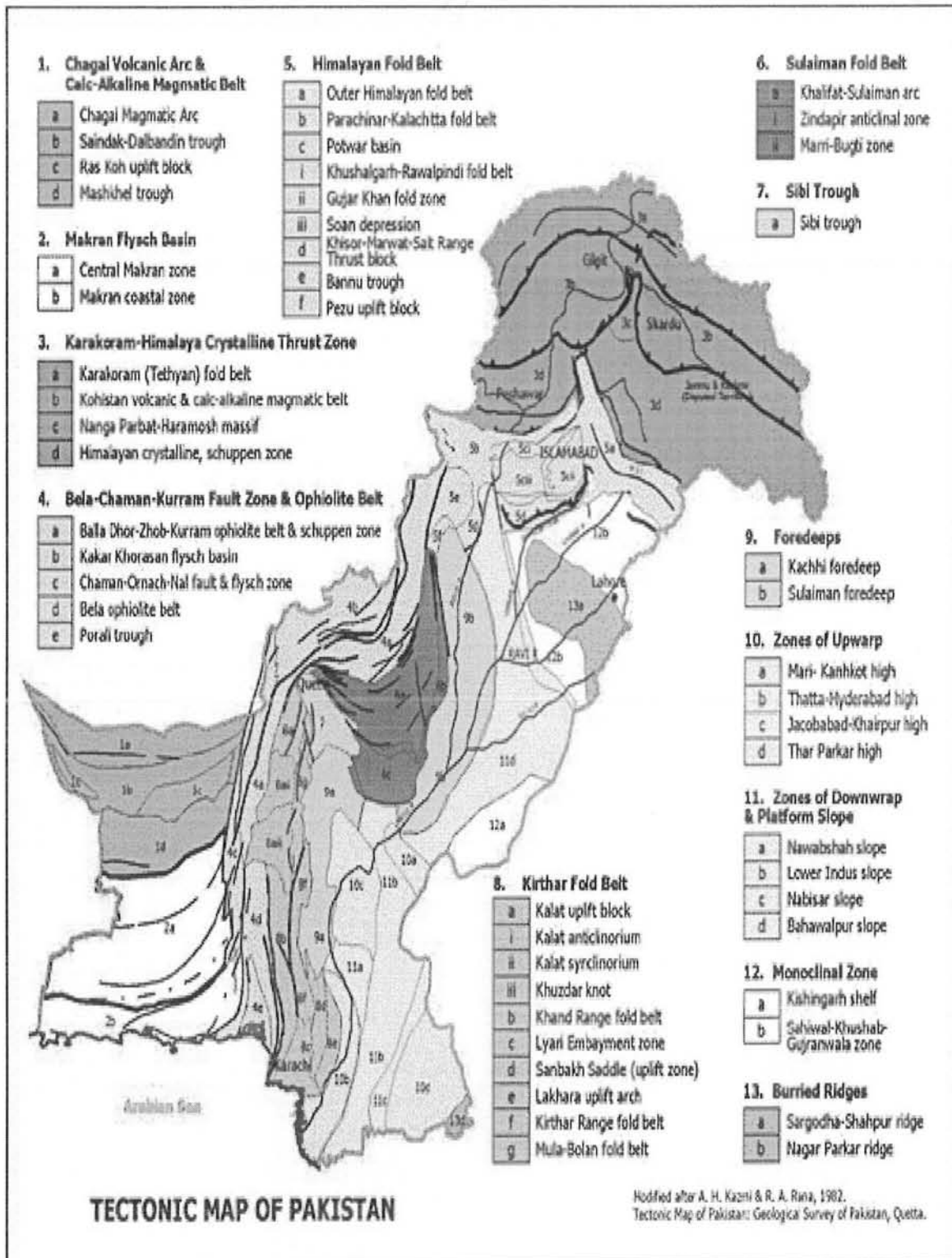


Figure 2.2: Tectonic map of Pakistan (www.gsp.gov.pk).

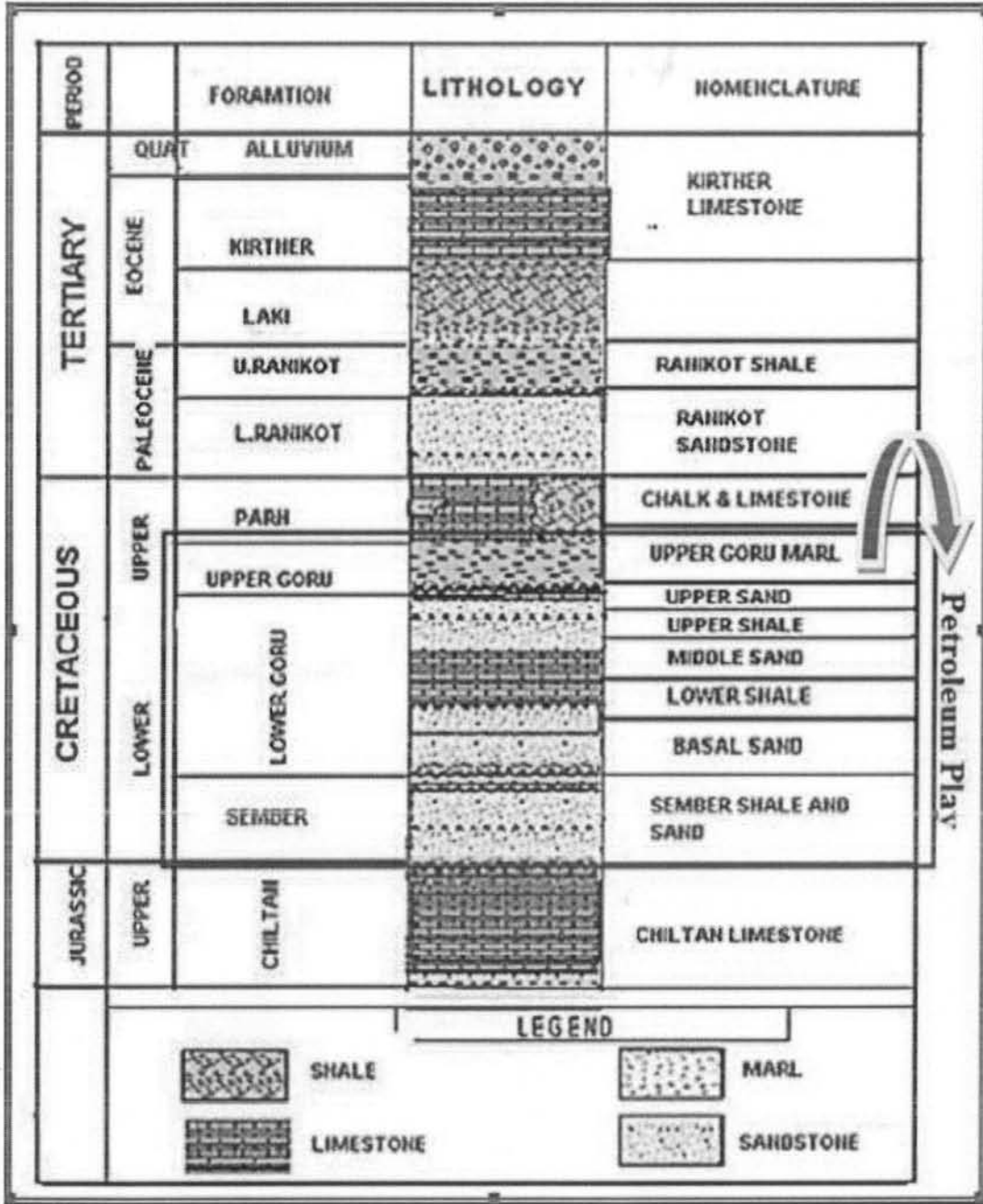


Figure 2.3: Generalized stratigraphy of the study area (Ahmed et al 1990).

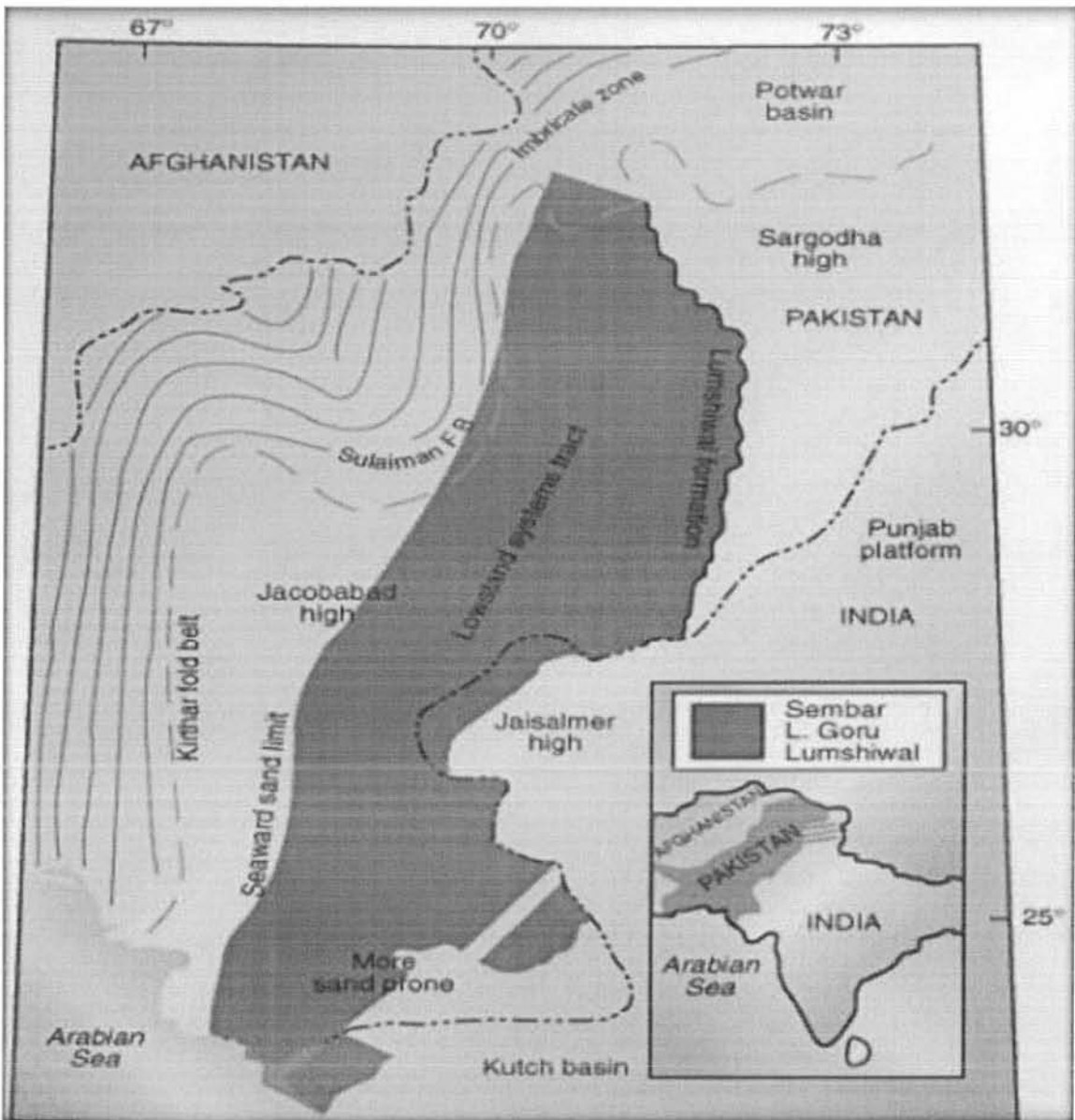


Figure 2.4: Petroleum play of Lower Indus basin (Stoneley, 1995).

3.1. Interpretation of 2D Seismic Data

Interpretation of the seismic section is done for the large area the area mostly done the structure interpretation and marks the prominent faults. Reflector is marked where the reflector is strong and clear, in such a way sequence is marked. A fracture is caused in the subsurface caused by the tectonic force called fault. Faults are basically the discontinuities that are cause because of the tectonic forces (Bakker, 2002).

As the seismic data is interpreted, then we are able to interpret the subsurface geologic structure such that fault, fold, horizons and the stratigraphic analysis. This is done to get information for the deposits of the hydrocarbon. Structural Interpretation of 2D seismic data of Block-20 Miano area is deals in this chapter. On the basis of seismic data interpretation following analysis can be made.

3.2 Basic Work flow of Seismic Interpretation

Following are the major interpretation steps that are taken to interpret the 2D seismic data

- Preparation of the base map of the area
- Faults marking on seismic section
- Interpretation of the Horizons
- Fault polygons construction
- Preparation of the contour map
- Basic flow chart of geophysical interpretational processes is shown in Figure 3.1.

3.2.1 Area Base Map Preparation

The Base map is formed by loading the latitude & longitude of the study area into the interpretation software. The seismic data may be the 2D or 3D. This will comprise the dip and the strike lines according to the structure of the area. The wells in the study area are loaded and displayed on the base map in Figure 3.1.

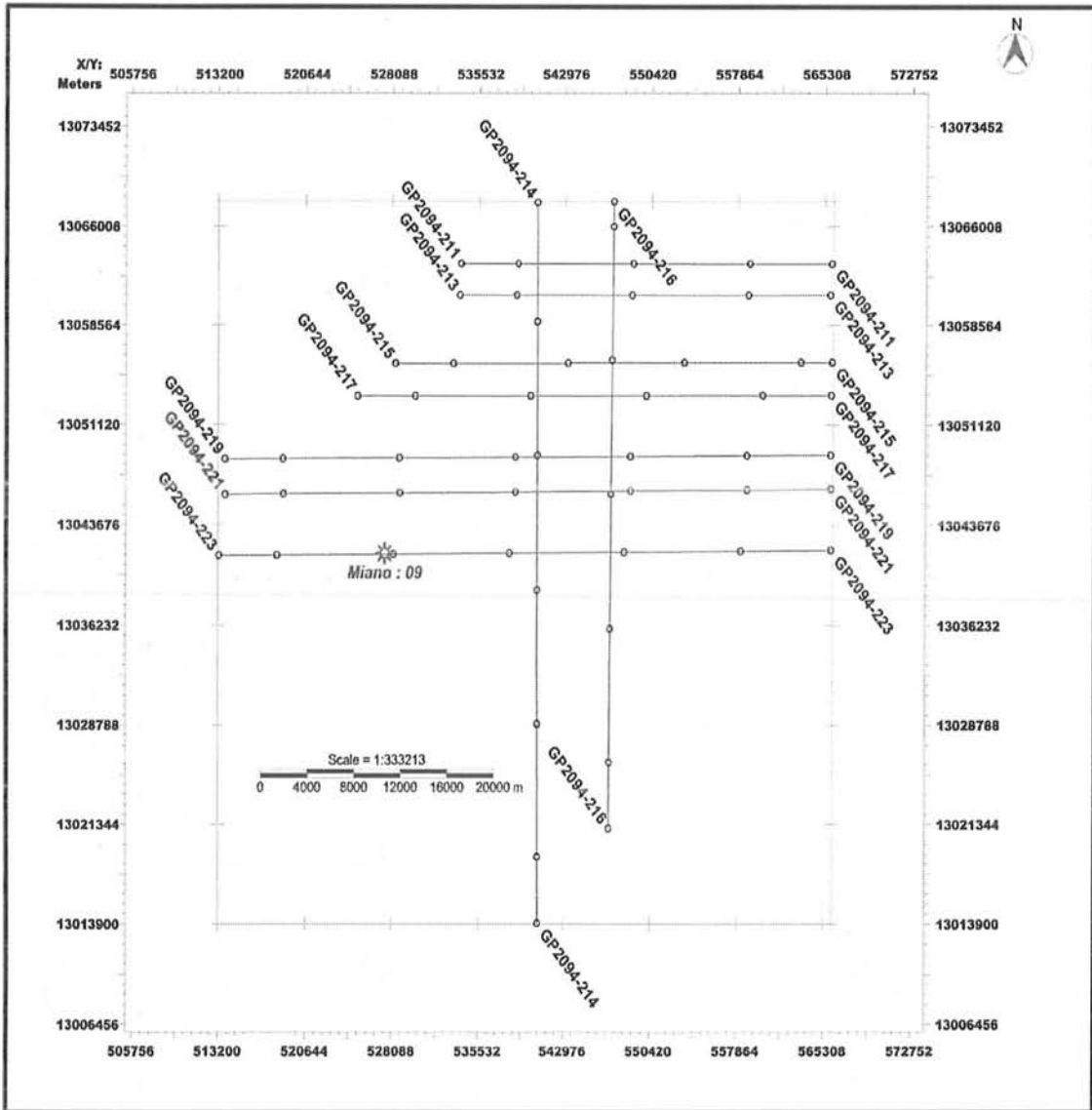


Figure 3.0: Base Map of Miano Area

3.2.2 Marking of Faults on Seismic Section

Faults are interpreted on seismic section where there is certain discontinuity or breakage in the beddings. Certain steps are necessary to identify the faults in the study area. The steps are

- Geology of area
- Faults correlation

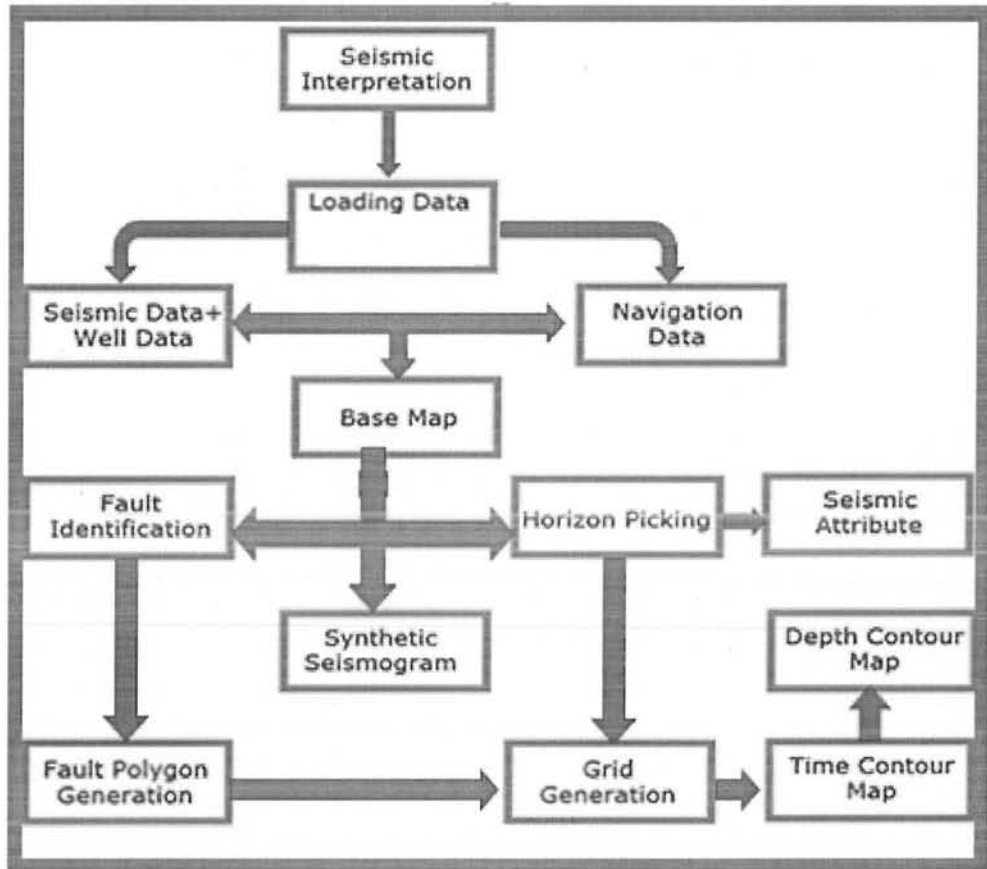


Figure 3.1: Flow chart Seismic Interpretation

3.2.2.1 Geology of Area

The study about the stress regime like compressional or tensional helps us to identify the patten of the faults. Mostly in compressional regime reverse faults are dominant with minor normal faults but in extensional regime we observe normal faulting. Also previous knowledge of study area helps about the age of the faults so primary and secondary features are easy to understand. Miano area is extensional regime where we observe horse and graben structures.

Major fault extend into the basement while splays along the major fault terminate to it. Geology of the area is important to purpose us the possible structure of the area.

3.2.2.2 Fault Correlation

The extension of the fault can be defined with the help of the fault correlation. It also defines the heave and throw of the faults and also network of the fault from where it passes through the different formation.

3.2.3 Horizon Interpretation

Interpretation of different horizon on the seismic section is the basic task of seismic data interpreter. The interpreter should have knowledge about the structures present in the area and also about the stratigraphy. The well tops are correlated with the seismic to mark the exact location of the horizons on the seismic section. On the basis of well tops of Miano-09, three horizons are interpreted. The names of these horizons are:

- Lower Goru Formation
- C-sand
- B-sand

3.2.4 Construction of Fault Polygon

The faults are interpreted on many sections so the faults correlate with each other and also to generate the fault polygon. The polygons can be constructed Manually and the Auto-generation.

3.2.5 Contour Maps Preparation

Final stage of Interpretation is the contour map generation. Contours are lines that join the points of equal time, elevation or depth. For contour map, Grid of the horizons is generated and then contour is generated on such a Grid. In seismic interpretation, first we prepare the TWT contour maps and then depth contour maps are prepared.

Three seismic horizons are marked on the seismic lines. These horizons were marked through the same steps and all the section are correlated at their respective tie points. The reflectors are strong enough to be picked because contrast in the acoustic impedance that is ultimately caused by changes in lithology. Normally the VSP data is used for naming the marked. In this study, six prominent reflectors are marked other wells of Miano area.

3.3 Seismic Tie

After marking horizons on a seismic section the next step is to tie the seismic section with the other intersecting seismic lines of the area. In this study horizons on the seismic line GP2094-221 are marked first because it is nearer to the well Miano-9. The tie points of the lines are confirmed from the base map, where tie points of the lines have been mentioned. At the tie point of both intersecting seismic lines have same horizons at the same time. If the horizon does not have same time then there may be miss tie that may be removed later on. Taking seismic line P2094-223 as a reference line, all other seismic sections used in the study are marked. At the tie point we not only mark the horizons but also mark the points of faults are also marked in the same manner all the faults were correlated.

3.4 Seismic Interpretation

In the first step the prominent reflector are picked and correlated with the well tops of miano-09 and the reflectors are identified. Also the lines are correlated with the synthetic seismogram of this well. Using tie of seismic lines from P2094-221 the other lines used in the study are marked. Three horizons are marked on the seismic section that is used in the study area and the horizons are named, with the help of the well data. The marked Horizons are assigned with different color. Horizon 1 is the Top of lower Goru Formation of Cretaceous age (green). Horizon 2 is the C-interval of sand in lower Goru Formation (orange). Horizon 3 is the B-interval of sand in lower Goru Formation (red). Throughout the study color scheme is kept constant for each horizon. The direction of deposition is east to west in the study area so the EW trending lines are dip lines and the structures (faults) are clearly observed on these lines. The NS trending lines are strike lines and on strike lines the faults cannot be clearly observed so the fault tie points from dip lines were highlighted on these lines. The base map of the lines used for the study along with the well location is shown in Figure 3.2. Numbers of normal faults are

marked on the seismic lines but there are two major horst structures as the area is in extensional regime. All the horizons are marked in manual picking mode in SMT Kingdom software.

The seismic lines P2094-219 and P2094-221 are the dip lines. All of the above mentioned horizons are marked as shown in figure 3 and figure 4 normal faults are marked on both the section forming major horst structures. Five are the major faults. The time of the horizons on seismic sections is given as; Top of Lower Goru is at 1.61 to 2.089 seconds. The time of horizons increases from west to east and so is the thickness of horizons, which indicates that the direction of deposition in the area is from west to east.

The horizons marked on the five faults are marked forming a graben. The interpreted seismic sections of the lines P2094-219 and P2094-221 are shown in Figure 3.3 and Figure 3.4 respectively.

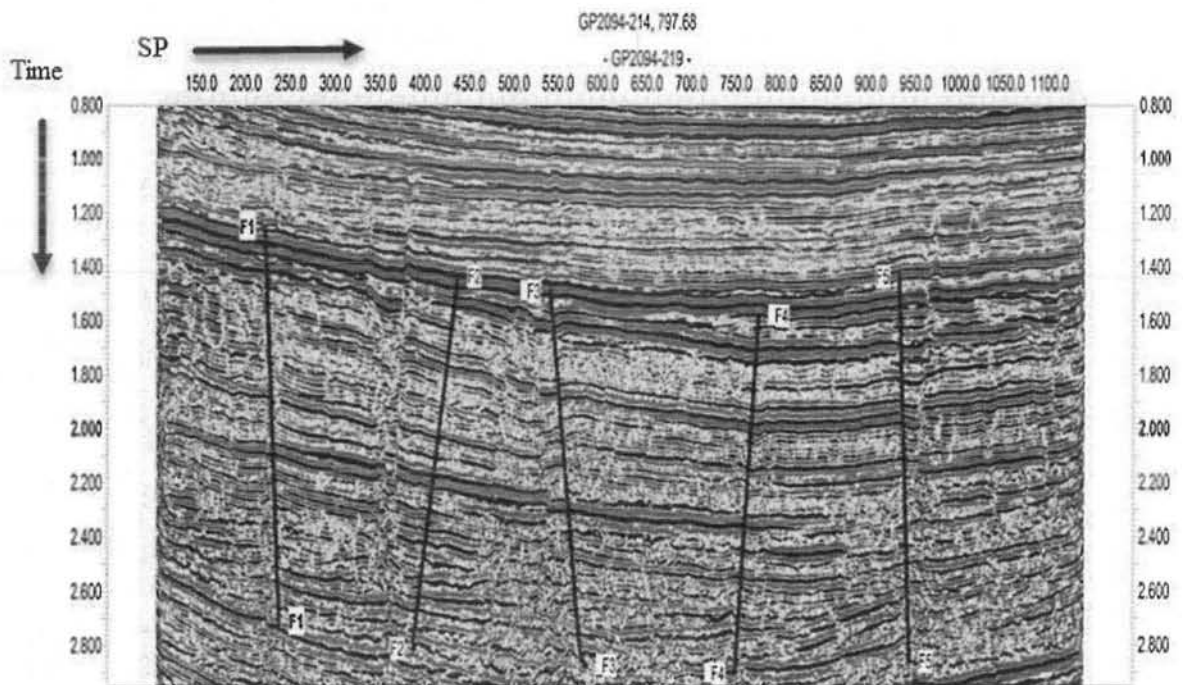


Figure 3.2: Interpreted seismic section of GP-2094-219.

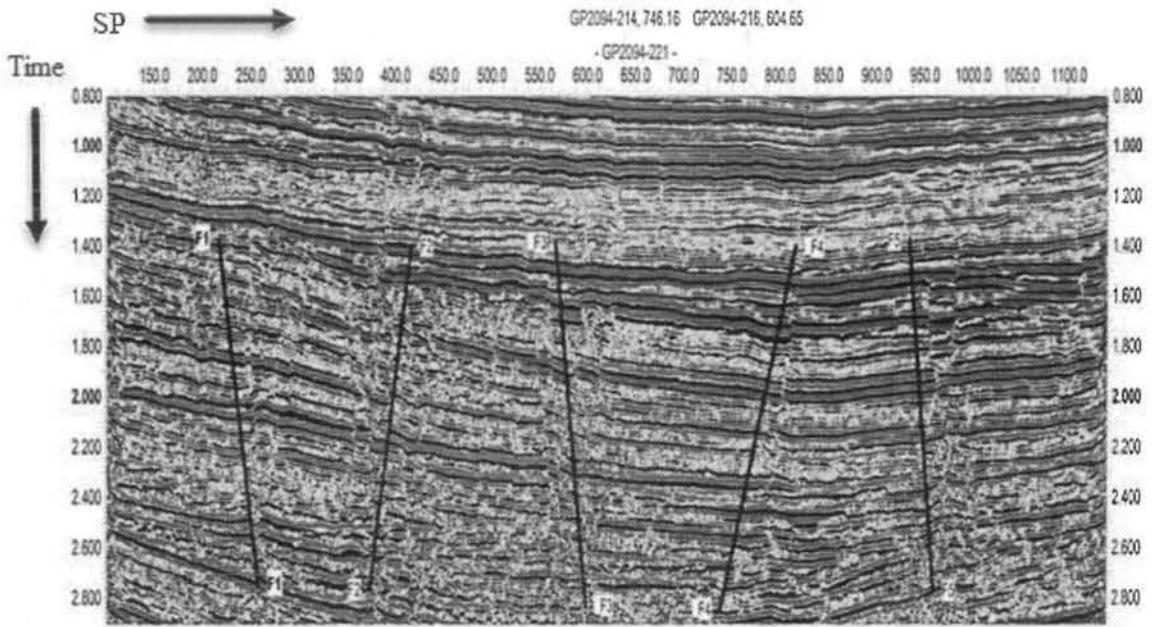


Figure 3.3: Interpreted seismic section of P-2094-221.

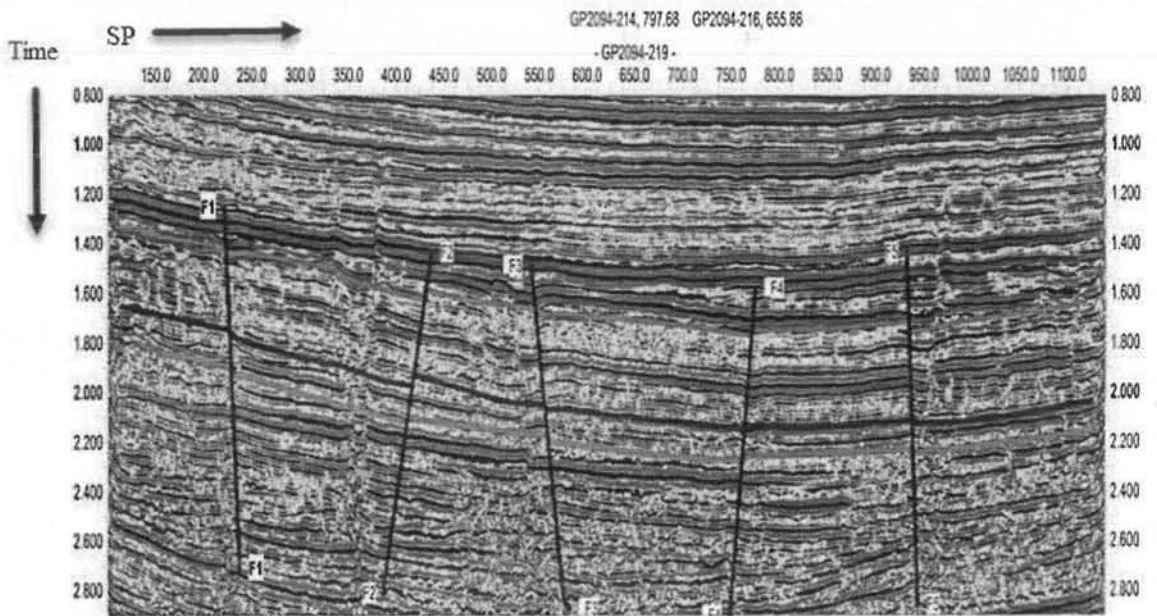


Figure 3.4: Interpreted seismic section line P2094-219.

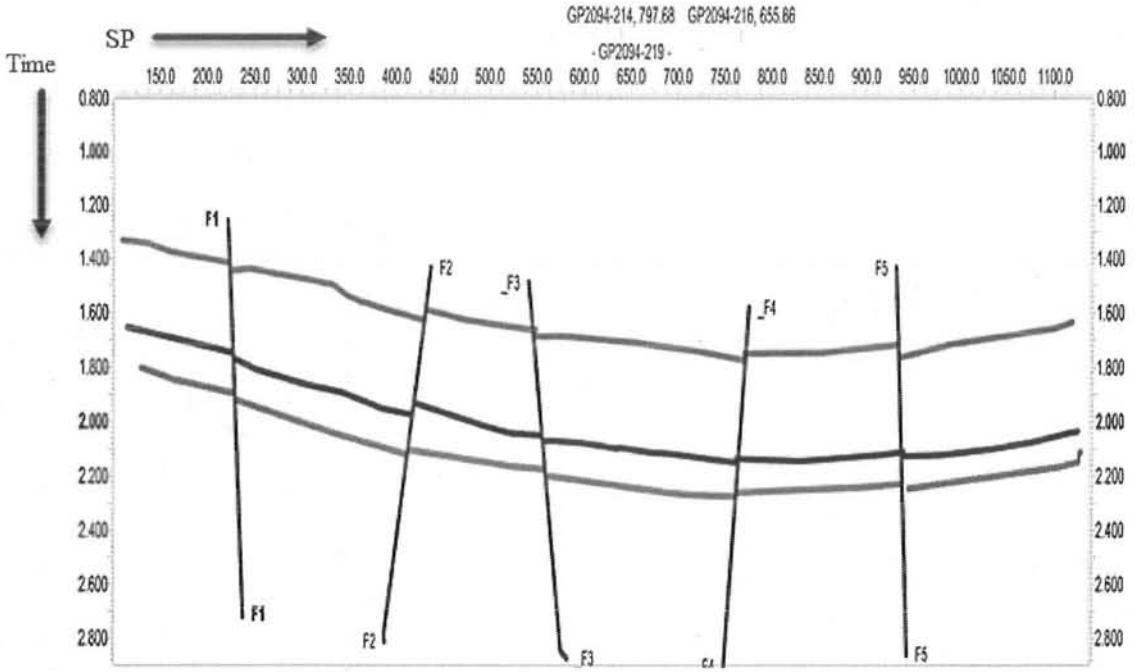


Figure 3.5: Interpreted cross section line P2094-219.

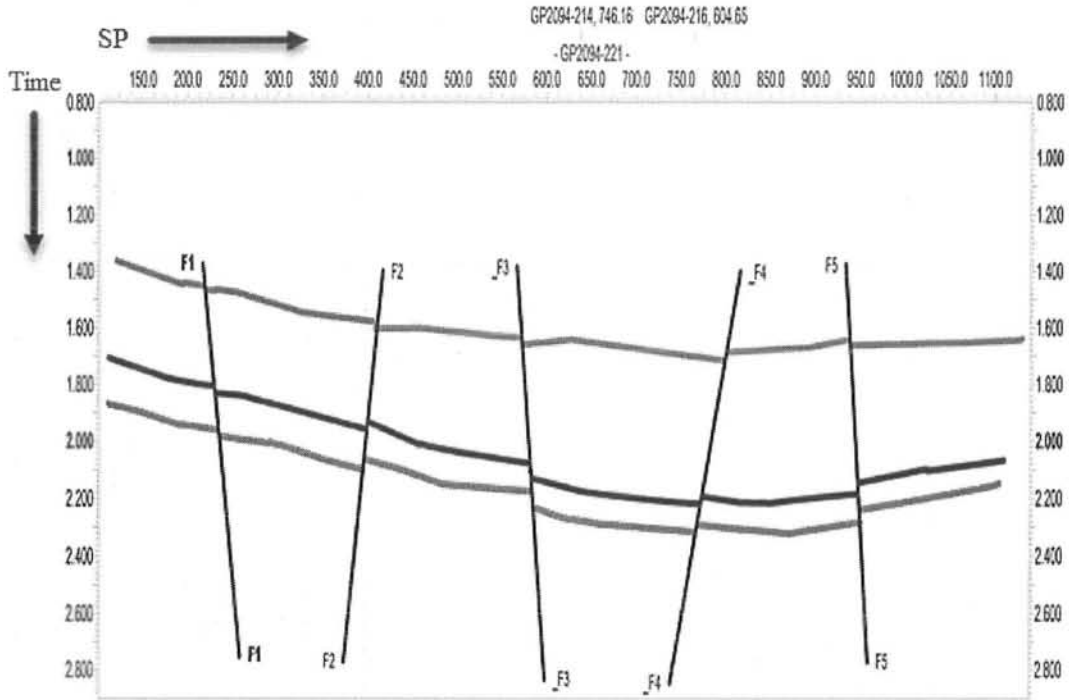


Figure 3.6: Cross section view of GP2094-221.

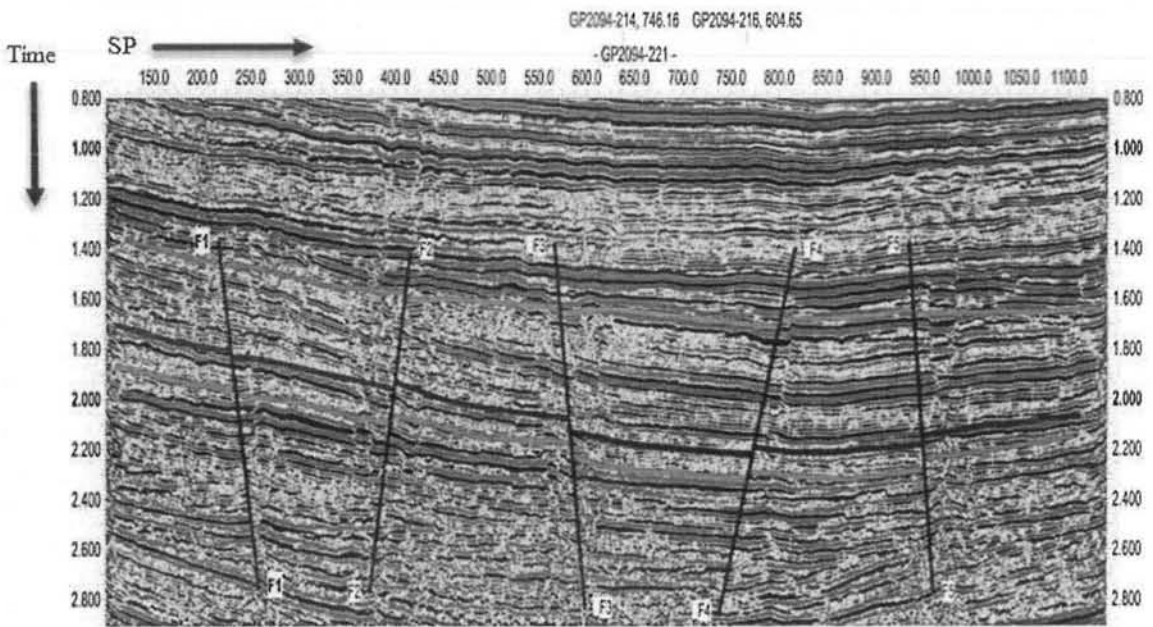


Figure 3.7: Interpretation of seismic lines P2094-221.

3.5 Time Contour Maps

Time contour map gives the information about the subsurface structure. It cannot show the structure directly but gives the idea about the structure and also give the information about the horizons. The contour maps are generated by the HIS Kingdom software. The time contour map for the B-interval and C-interval is generated.

3.5.1 Time Contour Map of B & C intervals:

TWT contour map of the B-interval and C-interval has been prepared with contour interval of 25 milliseconds (0.025 seconds) as shown in Figure 3.8 and 3.9. Five major faults F1, F2, F3, F4 and F5 are considered in mapping. F1, F3 and F5 have dip direction NW-SE while F2 and F4 have dip direction of NE-SW. These faults are normal faults making the geometry of horst and graben. F3 and F4 are the left and right lateral faults making the horst and graben for the B and C intervals. Those kinds of geometries represent the favorable sites for potential zones. The Figure 3.8 & Figure 3.9 represent that there is very minor throw of the faults. The contours which are observed in the time contour map for the B-interval start from 1.679s to 2.386s and for C-interval the contour start from time 1.537s and last contour has time 2.267s. Time contour map shows that B & C interval are shallower in the West and deeper in the East. As the contour time increases the response of the reflection is from the larger depth rather than the contour having the smallest time. The main objective of the time contouring is to get information about undulation in the time horizon due to folding and faulting.

3.6 Velocity analysis

Velocity analysis has been done to find out the average velocity within depth in the study area. RMS velocity is taken from the sections that are available in seismic section. From this RMS velocity, interval velocity and the average velocity is calculated and we find that there is 2300 meter per second is the average velocity that is in the B-Interval of the Miano area as shown in the figure 3.10.

3.7 Depth contour Maps

As the data is in the two way travel time, gives information about the subsurface structure. The depth contour map is prepared that truly related to the subsurface structure. Starting depth for B interval is 1930.530m and it ends up to 2743.805m depth. We have five faults having same directions as in the time contour maps. Formations are shallower in the West having depth of 1767.605m and deeper in the East with the depth of 2607.503m. Depth of the horizons is plotted against the Northings and Easting of the survey. Depth contour maps of the horizons are shown in the Figure 3.10 & 3.11.

3.8 3D view of the Fault Surface

We mark the fault on seismic line after this fault polygon is generated in Kingdom. Fault polygon gives us information about lateral movement of fault on the section view. In 3D view, we mark the dip where fault cuts it as shown in Figure 3.12 & 13. From the 3D view, in Figure 3.12 shows that faults cut the subsurface. This Figure shows two dips and one strike. While Figure 3.13 this will show the clear view about how contour are displace from the Fault place.

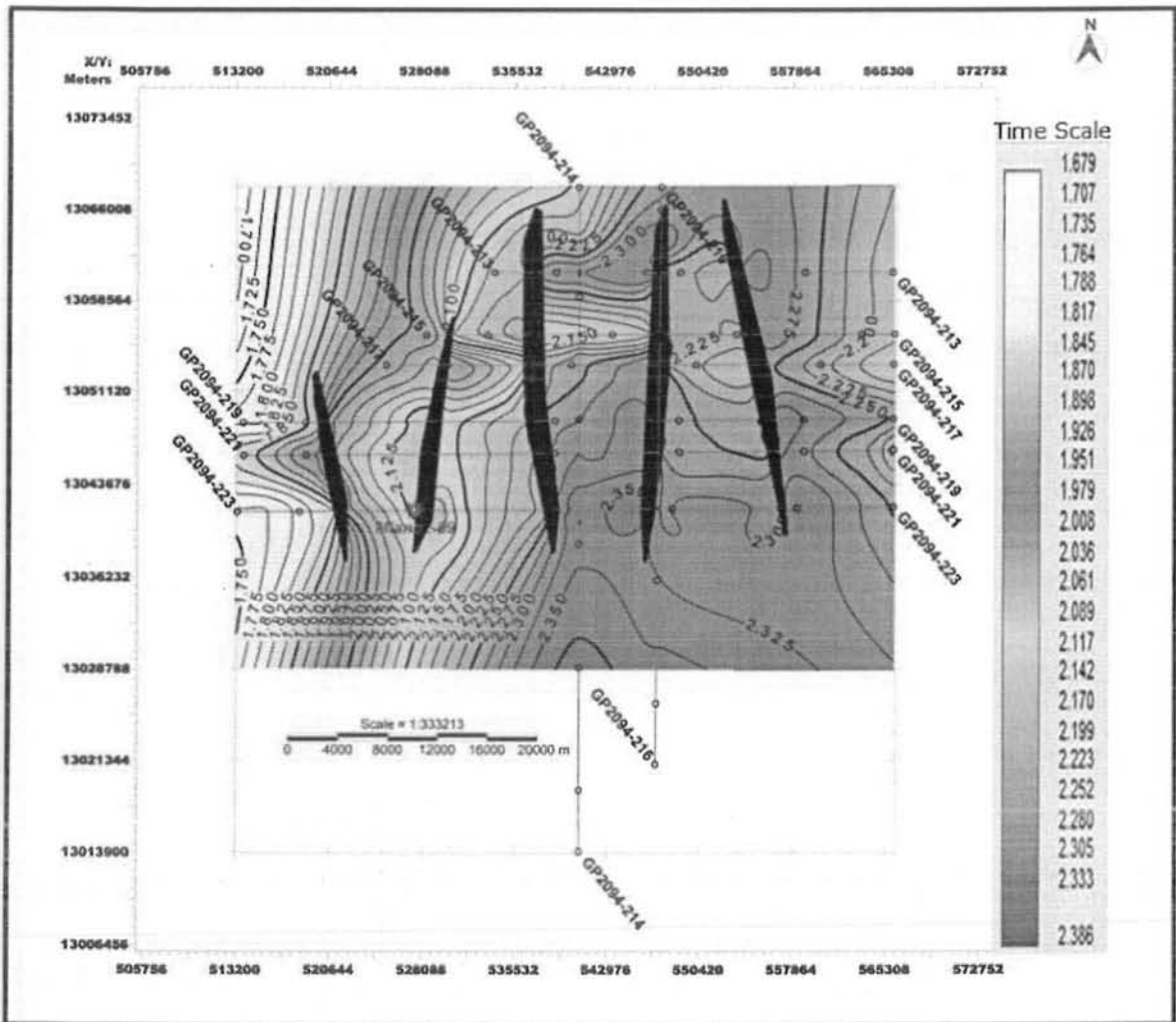


Figure 3.8: Time contour map of B-Interval.

3.9 Generation of synthetic seismogram

Synthetic seismogram is used for one dimensional forward modeling of the acoustic model energy traveling through different layers of the earth. Synthetic seismogram is generating for B interval and displayed in Well-09 on seismic line GP2094-223. Procedure followed for the generation of the synthetic seismogram can be summarized as, two way time for each well top is calculated by using depth, sonic well log and replacement velocity of the area. Figure 3.14 & 15 represents the generation of synthetic seismogram and its tie on seismic line. Map is obtained by using the following logs and ricker wavelet that is extracted from the log that are

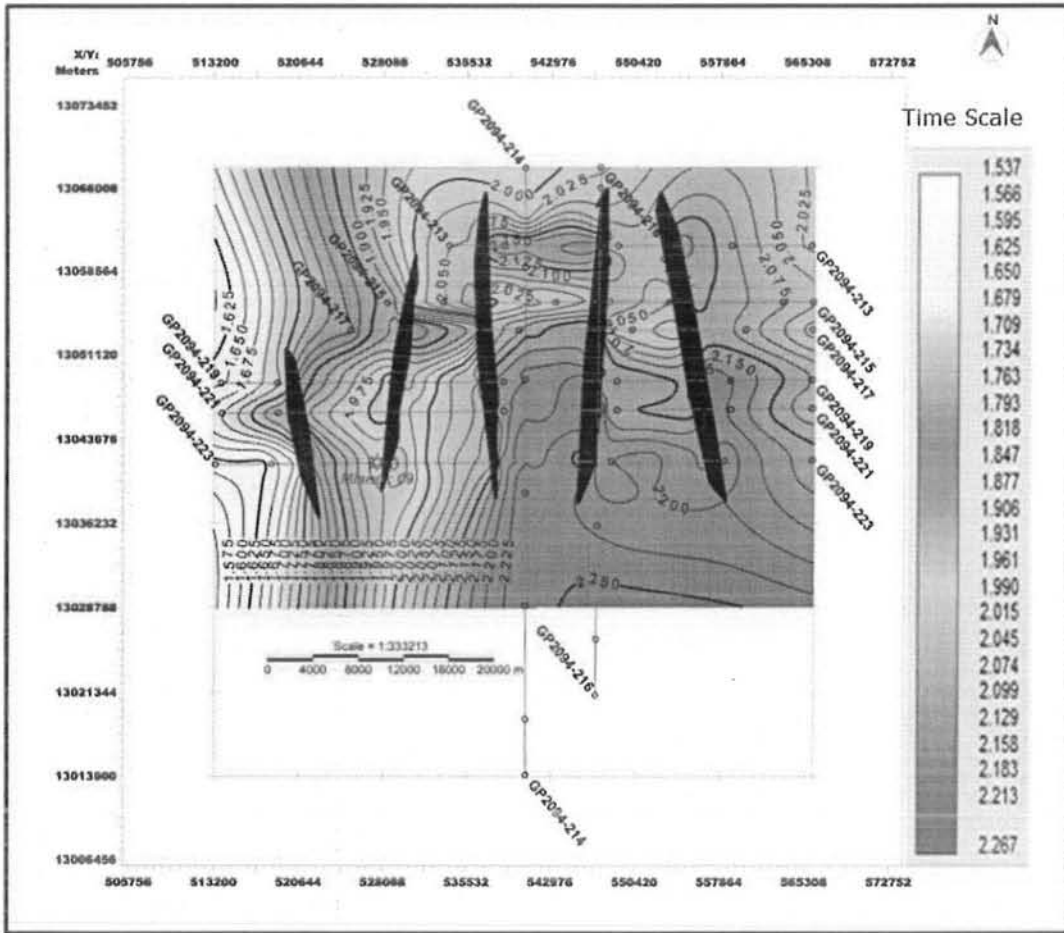


Figure 3.9: Time contour map of C-interval.

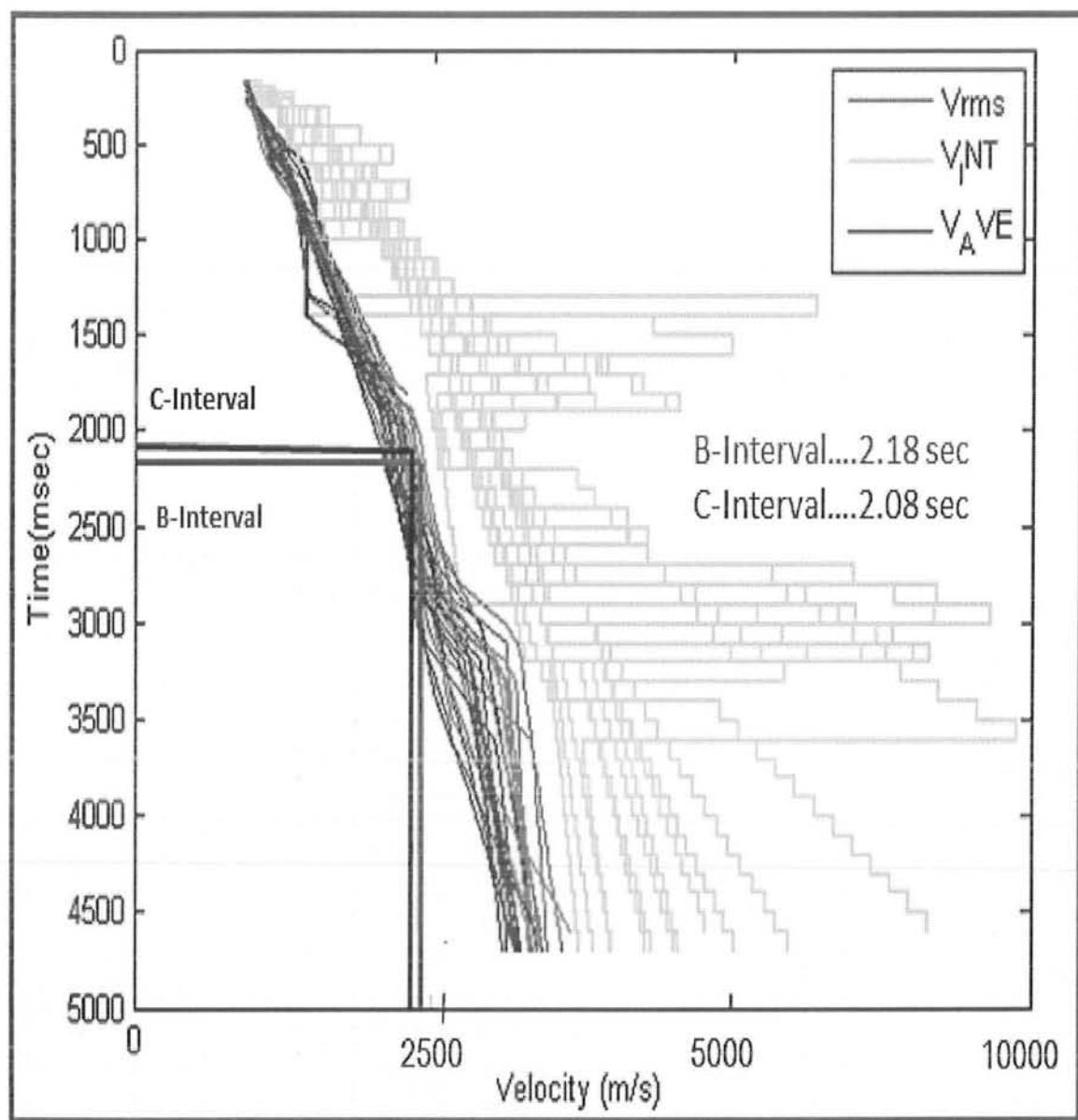


Figure 3.10 velocity analysis of the Lower Goru

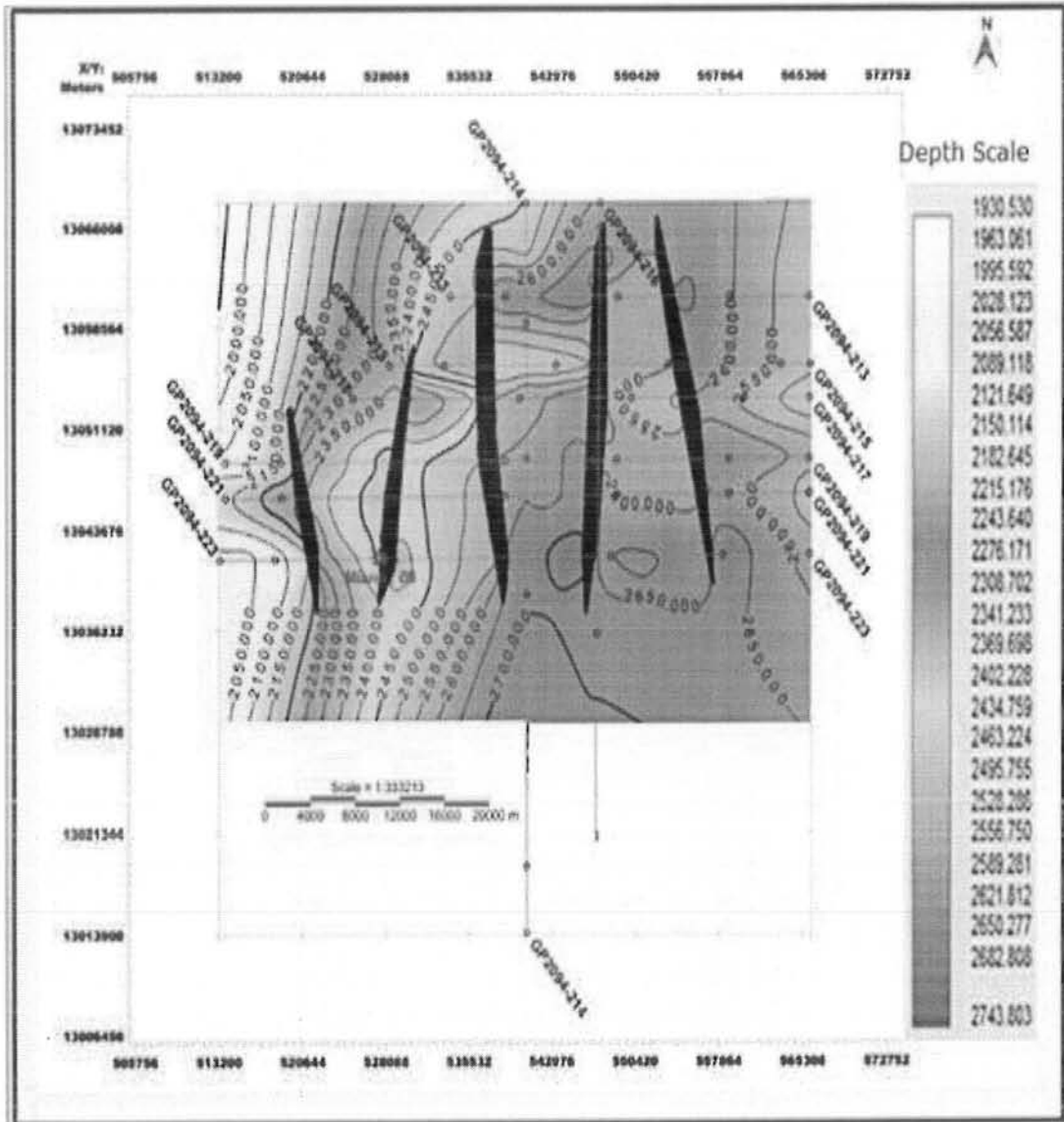


Figure 3.11: Depth contour map of B-interval

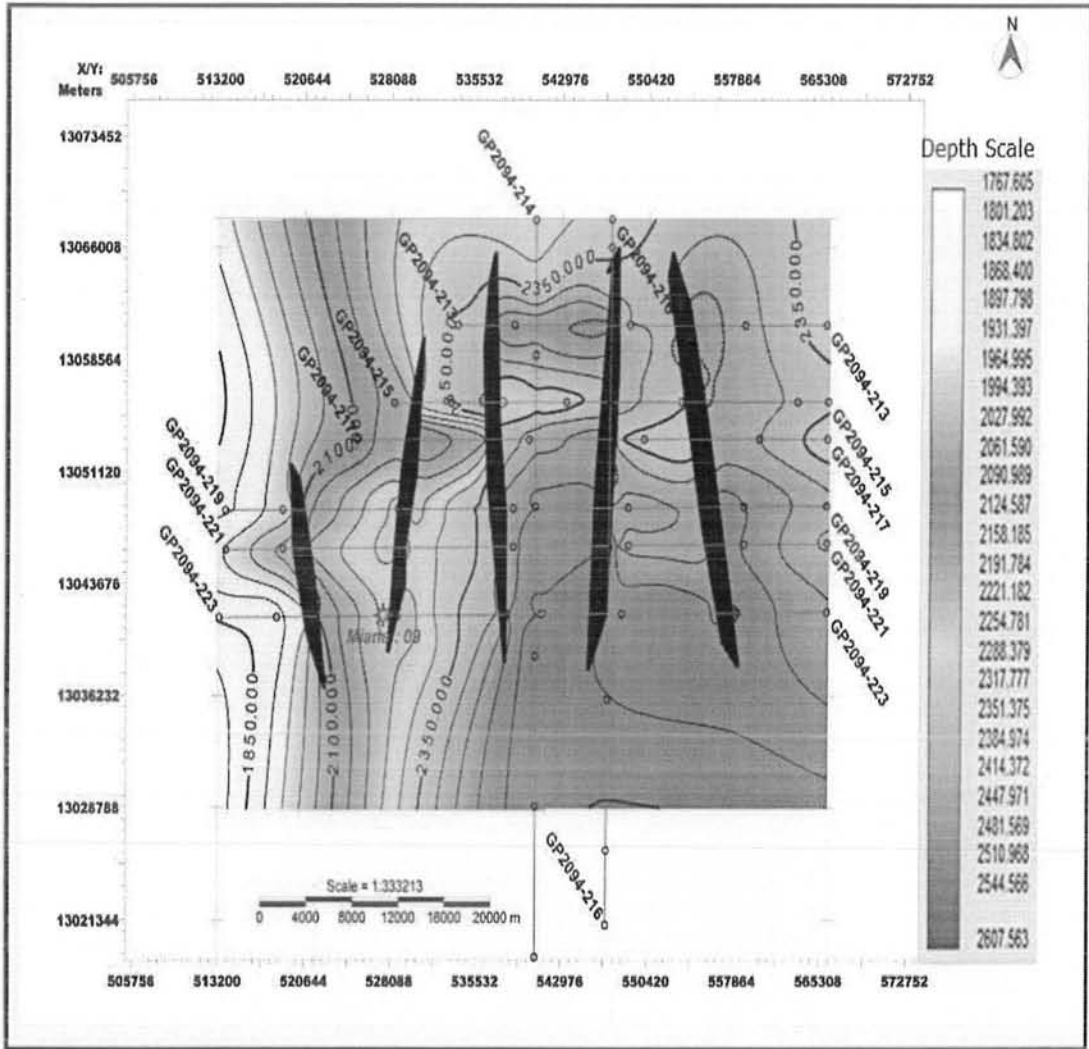


Figure 3.12: Depth contour map of C-Interval.

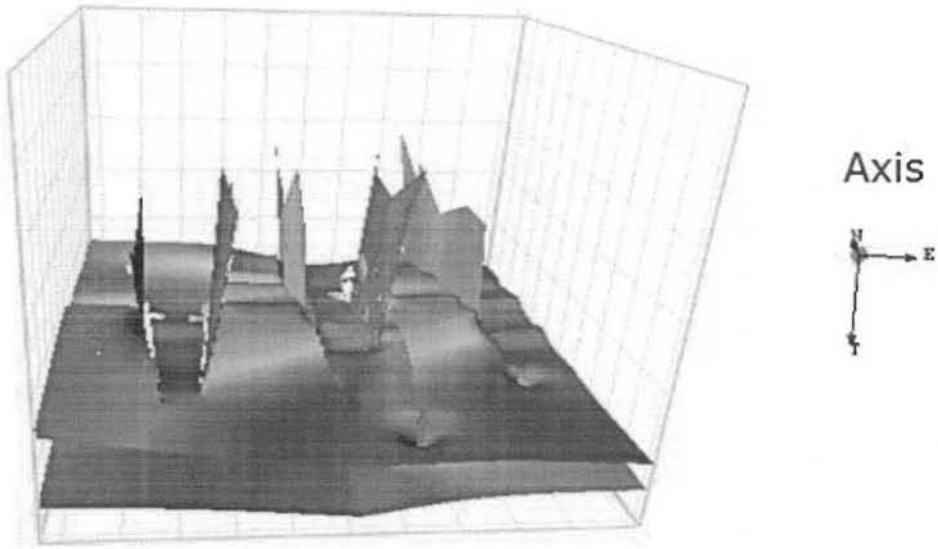


Figure: 3.13: 3D view of fault.

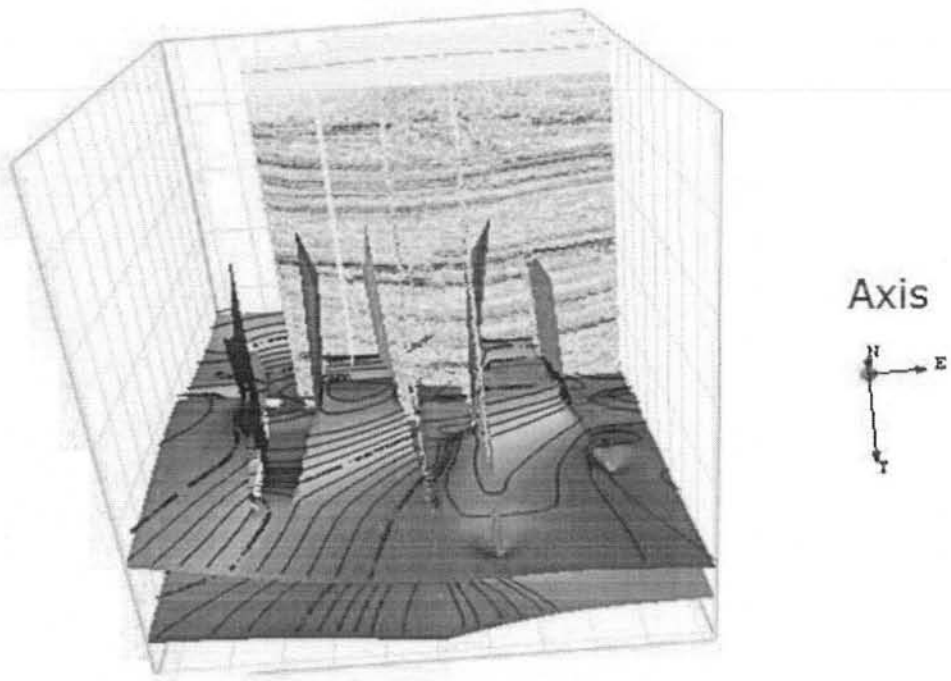


Figure 3.14: 3D view of Time contouring and Fault.

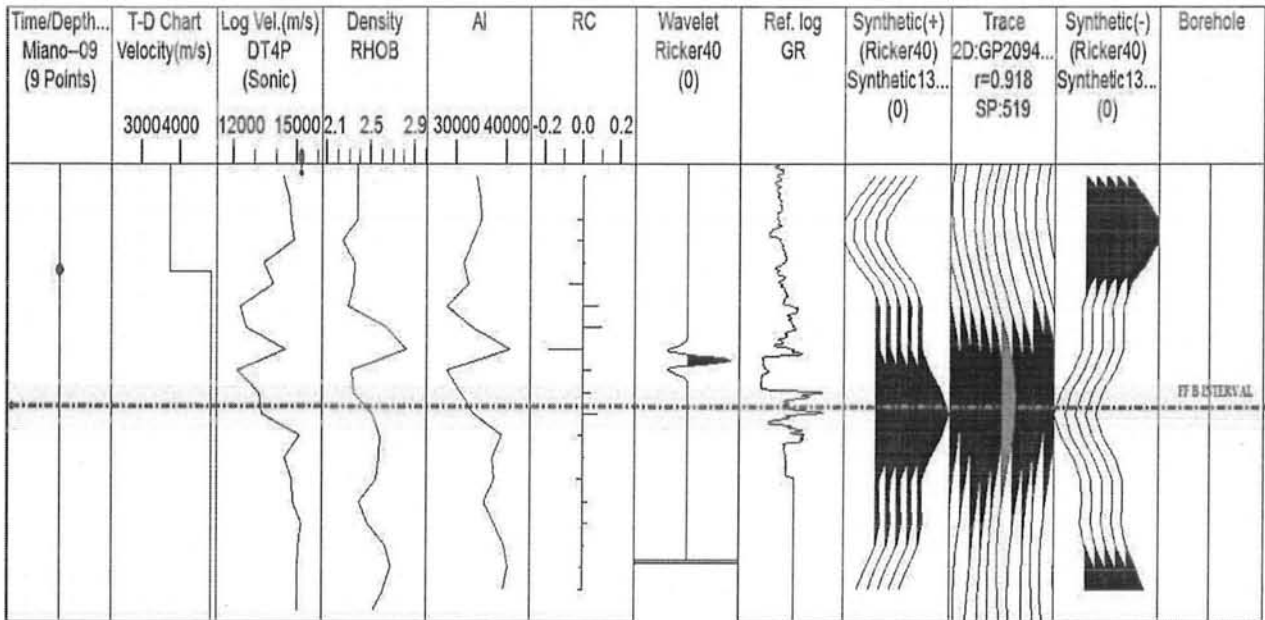


Figure 3.15: Generation of Synthetic Seismogram.

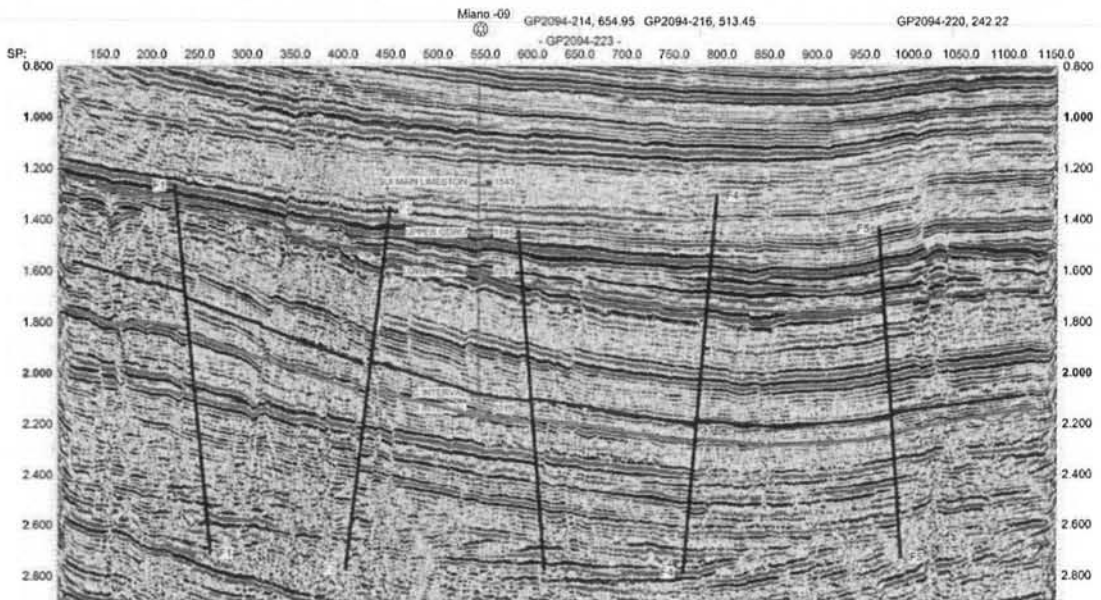


Figure 3.16: Display of synthetic seismogram on seismic line.

3.10 Seismic Attributes

Subrahmanyam & Rao (2008) have defined Seismic attributes as “*The seismic attribute are measured from the seismic data*”. Seismic attributes gives the information about the reservoir character and the different types of the attributes are used to get information about the lateral continuity and the discontinuity, (Subrahmanyam & Rao, 2008).

3.10.1 General Classification of Seismic Attributes

Different ways are, that shows the classified of the attributes. Several authors have given their own classification; according to Taner (2001) seismic attributes can be classified on the following basis.

Classification of Seismic Data Domain based:

- Attributes of Pre-Stack data
- Attributes of Post-Stack

Computational Characteristics based Classification:

- Instantaneous Attributes
- Wavelet Attributes

In this research work, seismic attributes are formed using seismic data domain based classification.

1)- Average Energy Attribute

Energy and the seismic attribute have the direct relation. Average energy attribute show the lateral continuity and the reflection strength. This attribute is apply on the 2D seismic line GP2094-219 (Figure 3.16). Discontinuity represent that there is a fault that is present.



Figure 3.17: Display of average energy attribute on GP2094-219.

2)- Envelope Attribute

Trace Envelope can be used as an effectively describe the following features

- The acoustic impedance contrast, hence reflectivity
- Gas accumulation, Bright spots
- Major variations in depositional environment
- Sequence boundaries
- Spatial relationship to porosity and other lithological variations

Attribute is applied on seismic line GP2094-219 (Figure 3.17) that clearly shows the reflectivity and also local and the major change in the lithology.

3) Frequency Attribute

This attributes provides the extra evidences about stratigraphy and reservoir. The frequency and the amplitude are inversely related and the point on the section upon which the

frequency attributes is applied, low frequency zone is marked as the reservoir. It is used as fracture zone indication and also for the hydrocarbon indicator. A cross section is generated (Figure 3.18) to show frequency variations with i.e. level of Lower Goru sands reflect low values of frequency.

4) Instantaneous Phase Attribute

Such type of the attribute is measured in degrees known to be the Instantaneous phase attribute. This attribute gives information about the continuity and discontinuity, relates to the phase component of the wave propagation and can be used to compute the phase velocity, (Subrahmanyam and Rao, 2008). The Instantaneous phase attribute that is applied on GP 2094-219 is shown in Figure 3.20

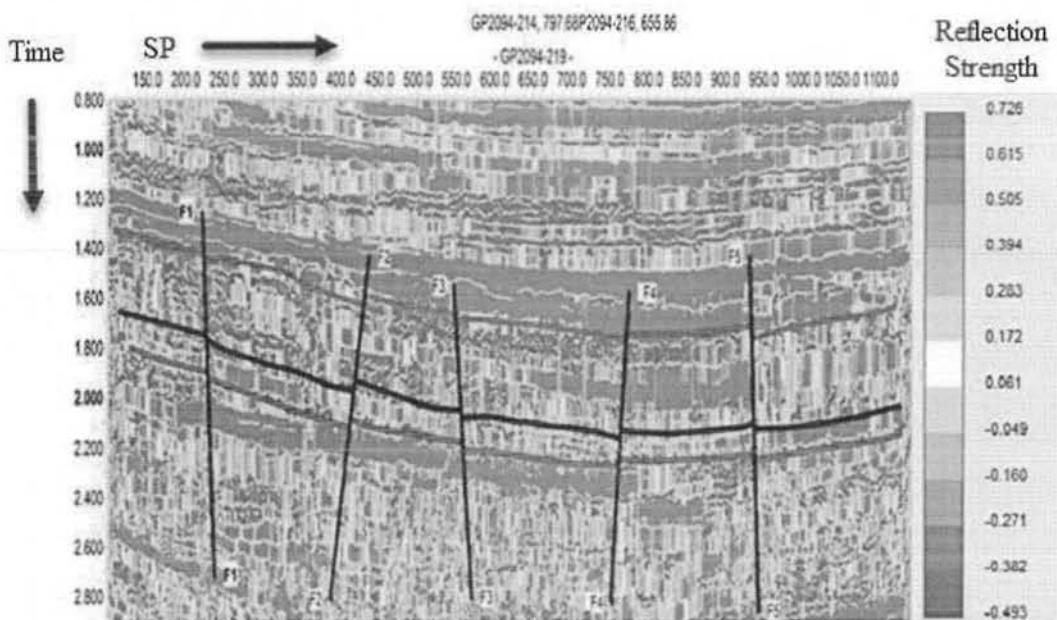


Figure 3.18: Display of Trace Envelope Attribute on seismic line GP2094-219.

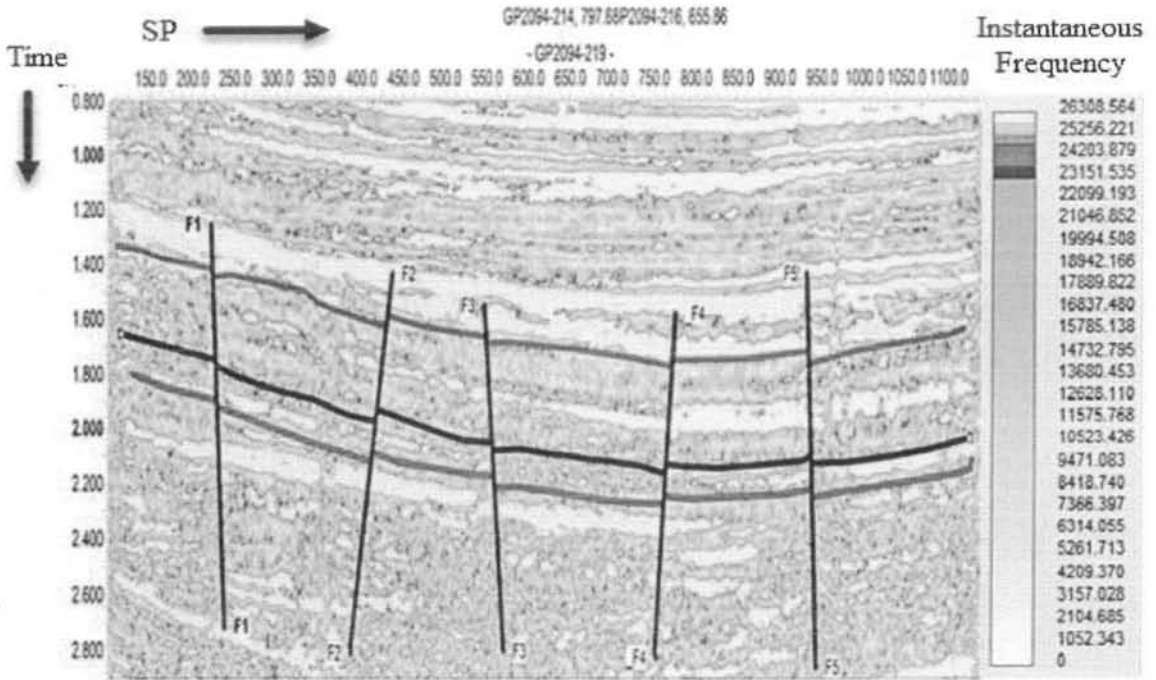


Figure 3.19: Display of frequency attribute on seismic line GP2094-219

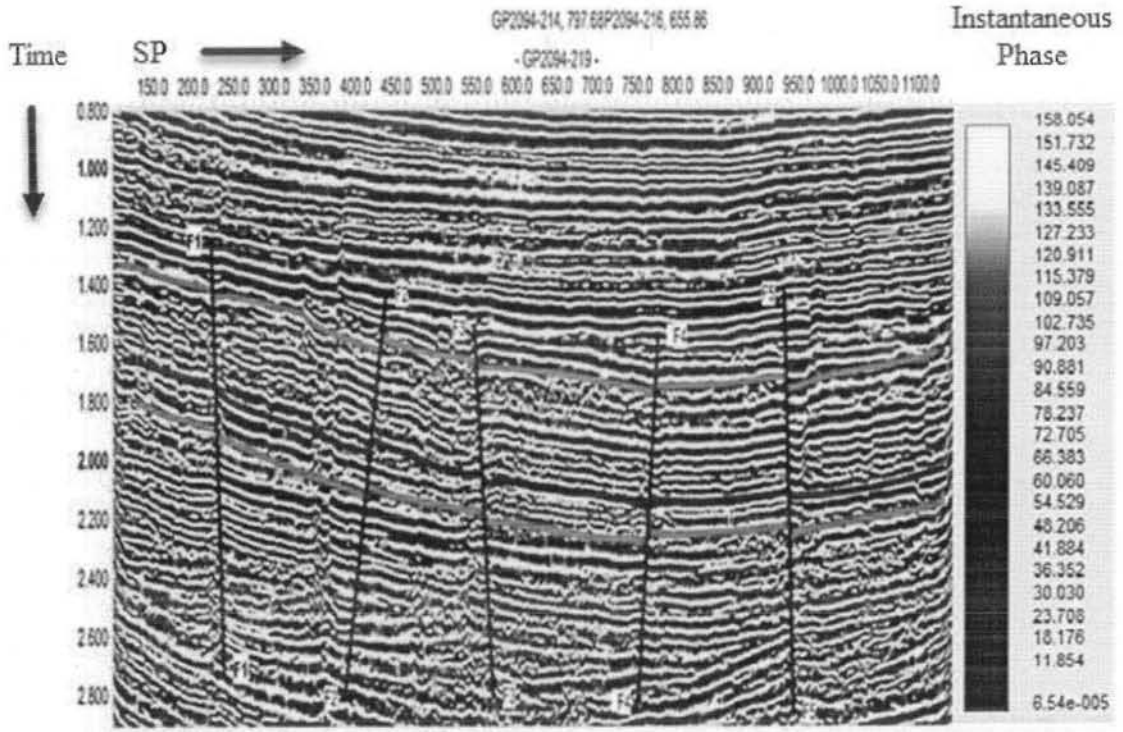


Figure 1.20: Instantaneous Phase of GP 2094-219

4.1 Introduction

Well logging is tool to measure the properties of the earth's subsurface. The study of the physical and chemical properties which are explained the presence and behavior of rocks, soils and fluids (Rider, 1996). Petrophysics uses well logs (caliper, resistivity, GR, DT, RHOB, Neutron logs etc.) and all pertinent information is obtain by use these well logs. Every well log has its own importance and these logs play very important role in quantifying the precise reservoir parameters such as porosity, permeability, net pay zone, fluid content and shale volume. Petophysical interpretation generally has less concern for seismic while more concerned with using well bore measurements to contribute to reservoir description (Krygowski, 2004).

4.2 Classification of geophysical well logs

Geophysical well logs can be classified into three categories

- Lithology logs
- Resistivity logs
- Porosity logs

4.2.1 Lithology Logs

Lithology log are mostly are mostly used to identify the boundaries between the permeable and non-permeable formation, information about the permeable formations provide lithology data for the correlation with other well logs.

Lithology logs are

- Caliper (CALI)
- Spontaneous potential (SP)
- Gamma Ray (GR)

a) Caliper (CALI)

Caliper logs measure the diameter of the borehole. It records the cavities where the well is caved in, and also the hardness of the rock cut during drilling. Where there is the porous material, mud cake will be formed that cause the hole diameter to become smaller. Variation in the diameter of the borehole influence the record of the different logs .Therefore it is important to consult with the caliper logs any artifacts (Knut Bjørlykke, 2010).

b) Gamma Ray Log

Gamma ray logs are used to measure the natural radioactivity of the formation. This is also known to be the lithology logs. The radioactive materials have high concentrations in

shale. Therefore shale free sand and the carbonates have low gamma ray reading. Volume of shale can be calculated by the following formula,

$$I_{gr} = \frac{GR_{LOG} - GR_{min}}{GR_{max} - GR_{min}}, \quad (4.1)$$

Where GR_{min} is minimum value and GR_{max} is the maximum value of the gamma ray, I_{gr} is the gamma ray index and GR_{LOG} represent the gamma ray log. Gamma ray logs are used to identify lithology, the volume of the shale and the correlation between the formations (Asquith and Krygowski, 2004).

4.2.2 Resistivity well logs

Resistivity well logs give the thickness of the formation, accurate value for the true formation resistivity and information for the correlation purposes. All these logs are plotted on the logarithmic scale due to more variation in resistivity (0.2 to 2000 ohm) with depth.

Resistivity well logs are

- Deep laterolog (LLD)
- Shallow laterolog (LLS)

a) Deep laterolog (LLD)

Deep laterolog is the electrode logs and are designed to measure formation resistivity in the borehole filled with saltwater muds (R_{mf}). The effective depth of the laterolog investigation is controlled by the extent to which the surveying current is focused (Asquith and Krygowski, 2004).

b) Shallow laterolog (LLS)

Shallow laterolog measure the resistivity of in the invade zone (R_i). In water-bearing zone, the shallow laterolog records a low resistivity because mud filtrate resistivity (R_{mf}) is approximately equal to mud resistivity (R_m), (Asquith and Krygowski, 2004).

4.2.3 Porosity well logs

Water saturation can be determined by the data that is provided by the Porosity logs. And also provide the accurate lithological and porosity determination and provide data to distinguish between oil and gas.

Porosity well logs are

- Sonic/Acoustic (DT)
- Neutron Porosity (NPHI)
- Density (RHOB)

a) Sonic/Acoustic (DT)

Sonic logs measure the interval transit time (delta t) of the compressional sound wave through the formation. The interval transit time is related to the porosity of the formation. The unit of measure is the microseconds per foot or microseconds per meter (Asquith and Krygowski, 2004).

Relation for the calculation of the porosity from the sonic log

Porosity of the formation can be calculated by using the following formula

$$\phi_s = \frac{\Delta t_{log} - \Delta t_m}{\Delta t_f - \Delta t_m} \quad (4.2)$$

Where ϕ_s represent the calculation that derived from the sonic log, Δt_m is the interval transient time of the matrix, Δt_{log} interval transient time of formation, represents the transient time of the fluid (salt mud=185 and fresh mud=189).the interval transient time of the formation depends upon the matrix material, its shape and cementation (Wyllie et al., 1956).If fluid (hydrocarbon or water) is present in the formation, transient interval time is increases and this behavior shows increase in porosity which can be calculated by using sonic log (Rider., 2002; Asquith and Gibson., 2004).

b) Neutron Porosity (Φ_n)

Neutron log is the porosity log that measure hydrogen ion (HI) concentration in a formation (Asquith and Gibson., 2004).In the shale free formations where the porosity is filled with the water, the neutron log is related to the water filled porosity (NPHI).In gas reservoir, porosity measured by the neutron log is low then the formation true porosity as the hydrogen ions concentration are less in gas reservoir then that of oil and water (Asquith and Krygowski., 2004).It is the one limitation of neutron log that is known as the Gas effect.

c) Density (RHOB)

Density log is the porosity log that measure electron density of the formation, (Asquith and Krygowski., 2004). Formation electron density is actually related to bulks density of formation. The density logs are used with other logs and also separately for different purposes (Tittman and Wahal., 1965).

Relation for the calculation of the porosity from the Density log (ϕ_d)

Density log can be used to find out the correct porosity of the formation, if the matrix densities in the formation or rock type are known (Asquith and Gibson, 2004). The rock type in my research work is sandstone and shale. By using following mathematical relation, density porosity can be related as

$$\phi_d = \frac{\rho_m - \rho_b}{\rho_m - \rho_f} \quad (4.3)$$

where,

- ϕ_d represent porosity derived from the density log
- ρ_b represent bulk density of formation
- ρ_m represent matrix density and for sandstone it is 2.65
- ρ_f represent density of fluid.

The main purpose of present petrophysics is to obtain calculation about porosity, saturation of water and hydrocarbon.

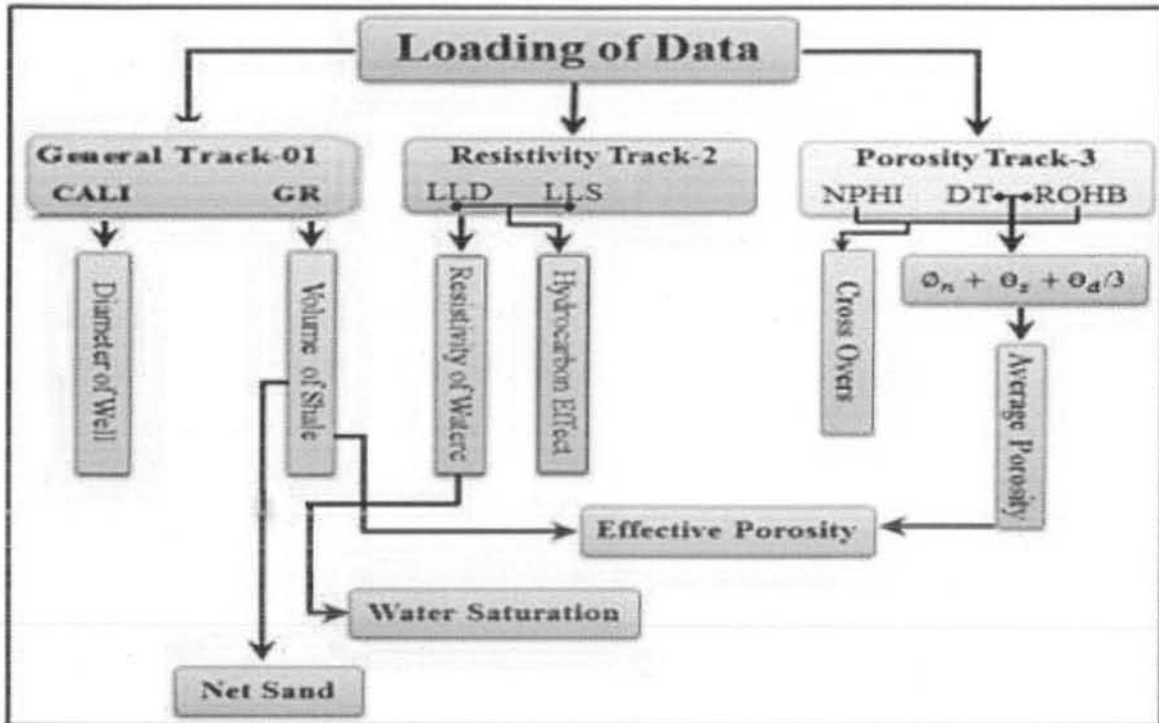


Figure 4.1: Methodology adopted for petrophysical interpretation.

4.3 Average porosity calculation

Sum of the porosities that are obtained from the different logs divided by number of logs from which porosity is calculated. Here Lower Goru formation is reservoir of cretaceous age for which the average porosity is calculated, to zone of interest reservoir, all the logs are interpreted. The relation is given below through which average porosity is calculated.

$$\phi_{avg} = \frac{\phi_n + \phi_d + \phi_s}{3}, \quad (4.4)$$

where,

- ϕ_{avg} is the average porosity calculated from the available porosities
- ϕ_n represents neutron porosity
- ϕ_d represent the density porosity

- ϕ_s represent the sonic porosity.

4.4 Effective porosity (ϕ_e)

This will define as “The ratio of the interconnected pore spaces to the total volume of the rock. The shale effect is removed from the rock unit”. The zone which rich in the shale, effective porosity will be zero. Effective porosity is used to mark the saturated zone. The effective porosity can be calculated by the following formula (Asquith and Gibson, 2004).

$$\phi_e = \phi_{avg} \times 1 - V_{sh} , \quad (4.5)$$

Where,

- ϕ_e effective porosity which to be calculated
- ϕ_{avg} represent the average porosity
- V_{sh} represent volume of the shale.

4.5 Mathematical relation for Water Saturation (S_w)

Water saturation in the formation can be defined as “The percentage of the pore volume filled by water in the formation”. The saturation of water in the formation can be calculated by the following Archie equation

$$S_w = \left(\frac{F \times R_w}{R_t} \right)^{\frac{1}{n}} , \quad (4.6)$$

where,

- F is formation factor which is

$$F = \frac{a}{\phi^m} \quad (4.7)$$

- R_w represent the resistivity of water
- R_t represent the true formation resistivity
- n represents the saturation exponent
- a is the constant and its value is 1 in case of sand
- ϕ represent effective porosity
- m represents the cementation factor and its value is taken 2 for the sandstone.

Mathematical relation for Hydrocarbon Saturation (S_h),

$$S_h = 1 - S_w \quad (4.8)$$

Hydrocarbon saturation can be defined as “the pore in formation is filled with hydrocarbon”. It can be calculated by using the following mathematical relation

Where S_w represent Hydrocarbon saturation, S_h represent hydrocarbon saturation.

4.6 Interpretation of well log

IHS Kingdom software is used for the analysis of Miano-09 well; within the depth Range of the B-sand 3331 m to 3390 m. Due to collapsing of wellbore Ruguosity effect will be occur. Therefore in the depth ranges, if there is Ruguosity, the value of the other log is not consistent. GR log, Caliper log are displayed in track-1.LLD and LLS log are displayed in track 2. DT, NPHI and RHOB are displayed in track-3. The crossover of NPHI and RHOB is important, if depth of NPHI is remain same but value of the RHOB is changed within that depth, it indicate fluid contact (Figure 4.2). Depth scale is shown in track-4. Volume of shale V_{sh} is displayed in track-5. Shale and sand can be separated by applying 40% cut-off value. Below this cut-off value, there is sand and above this cut-off, there is shale. Density porosity is displayed in track-6, calculated from DT4P.Average porosity (PHIT) is displayed in track-7 and actually is the sum of NPHI and DT4P divided by 2. Effective porosity is displayed in track-8 after removal of the shale effect. Water saturation (SW) is displayed in track-9 and Hydrocarbon saturation is calculated from the water saturation.

B-sand petrophysics is done to depth from (3331 m) to (3390 m).In this way, interest zone that called the reservoir is from 3338 m to 3346 m defined where sandstone is encountered. The calculation parameter is displayed in the table.

Table 4.1 Calculated parameters for B-sand in Miano-09 Well.

Serial Number	Calculation Parameter	Percentage % (3331-3385)m	Percentage % (3338-3346)m
1	Average Volume of Shale= $V_{sh_{avg}}$	44	24
2	Average Porosity Obtained From Density log= $\phi_{d_{avg}}$	11.3	18
3	Average Porosity in(PHIT) Percentage= ϕ_{avg}	11.8	12
4	Average Effective Porosity in Percentage= $\phi_{e_{avg}}$	6.4	8
5	Average water Saturation in Percentage= $S_{w_{avg}}$	51.7	38
6	Average Hydrocarbon in Percentage= $S_{h_{avg}}$	47.2	62

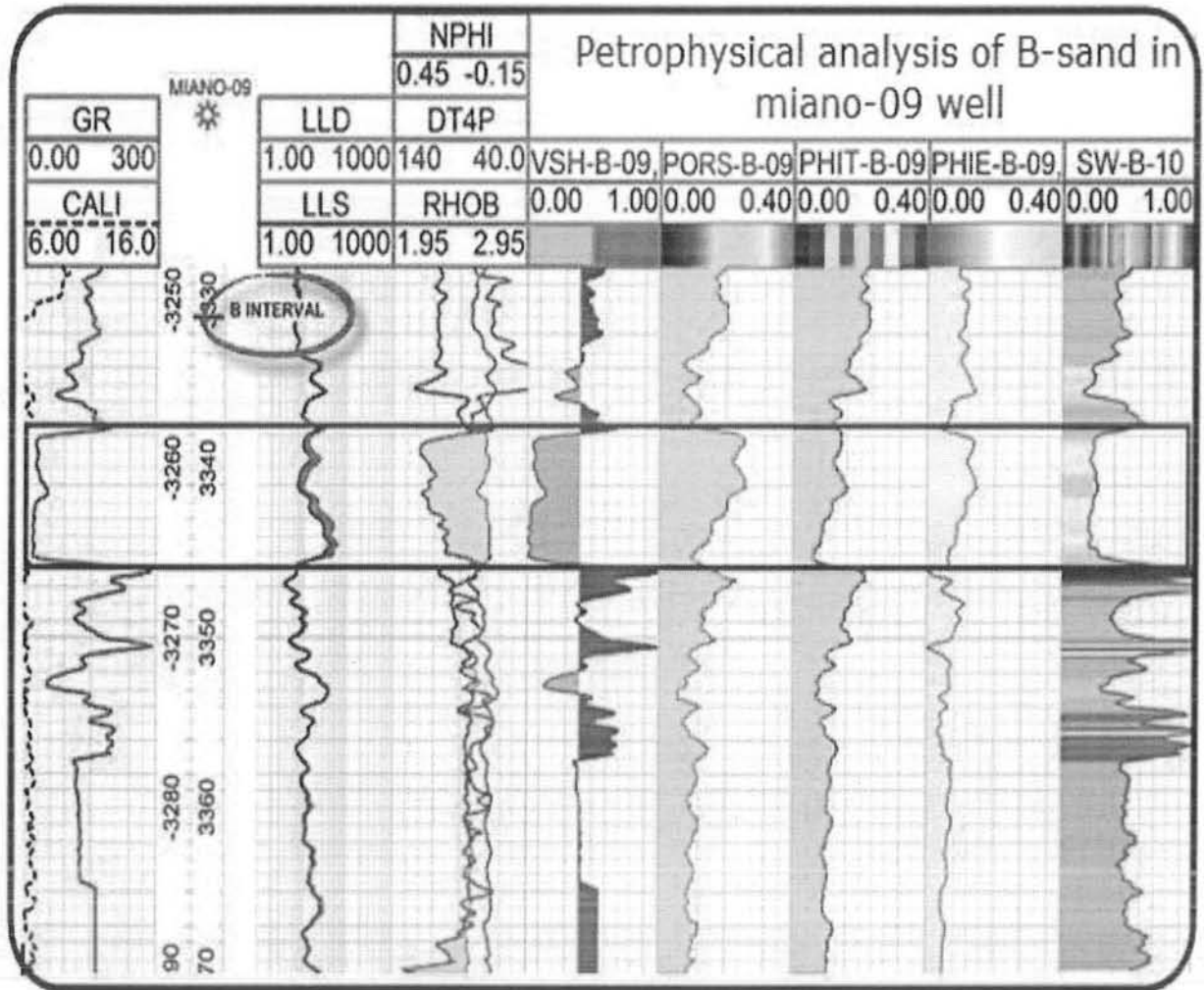


Figure 4.2: Petrophysical analysis of B-sand Miano well-09.

4.7 Rock Physical Relation:

Partial gas saturation is remain the lovely topic because of the question related to the seismic detectability. Undersatanding of the causes of partial gas saturation may help to avoid non.productive resevior. In figure 2 we discuss the influence of lithology on the partial gas saturation .The presense of the shale has influence on gas saturation and the rock elastic properties.

This is the accepted theory that small percentage of gas saturation, often within 10% , will cause drop in Vp velocity. Consequently, partially gas saturated resevior has been drilled mistakenly. (Domenico, 1976)

The resevior rock of the miano area has porosty , saturation of water ,mostly it consist of sand and shale. To eximine how lithology variation impact on the gas saturation , P_wave velocity, Volume of shale(V-SH) and related petrophysical logs are shown in figure 2. Dierct observation of the figure shows that the water saturation is directly related to the

Volume of shale, Porosity increases with decreases Volume of shale. The clean sand has high gas saturation and above that there is the low gas saturation as it consist of more voume of shale then the clean sand.

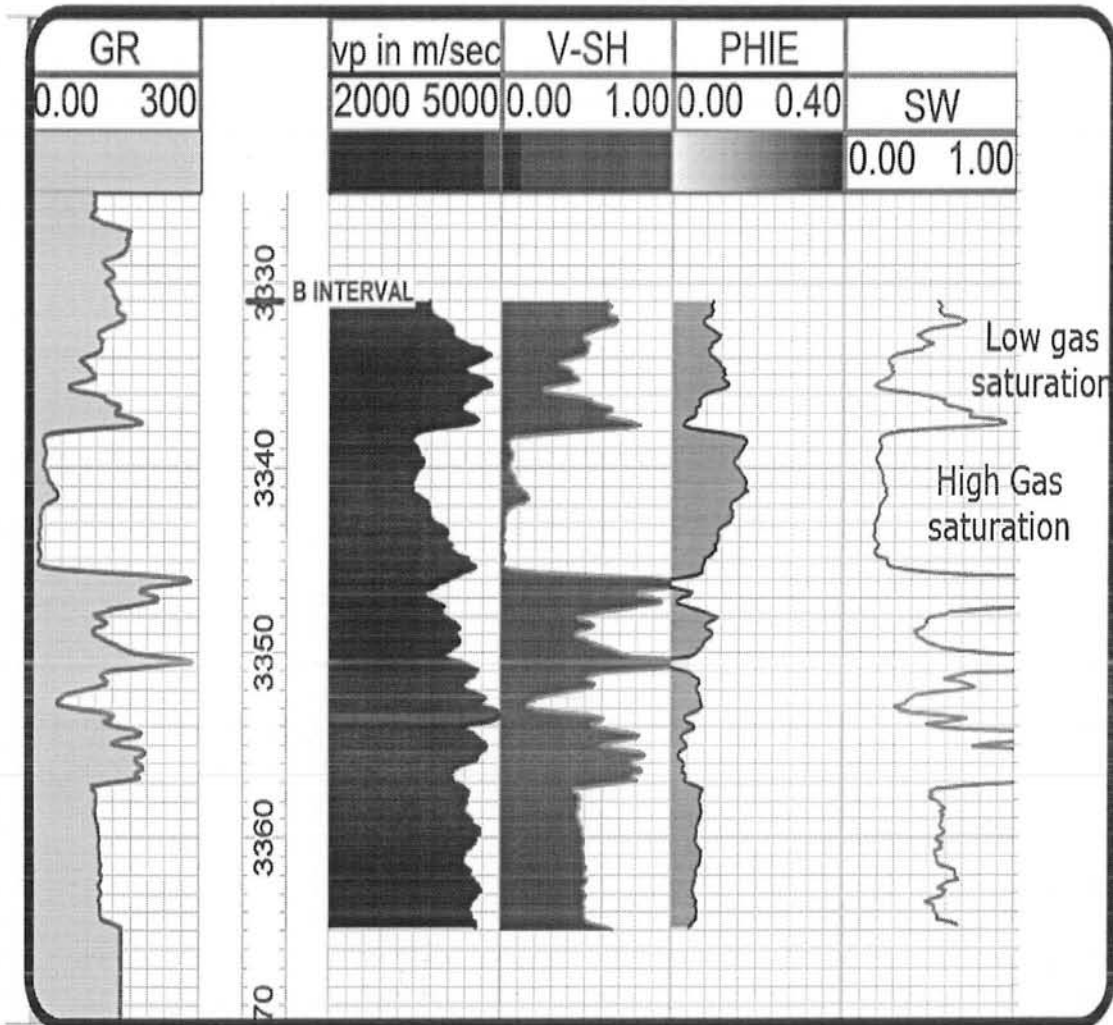


Figure 4.3: Petrophysical Rock properties of Miano well-09

4.8 Facies Analysis

Facies are considered to the body of the rock that exhibit specific characters but ideally they are rock units that are formed under some condition of sedimentation. An important contribution to subsurface analysis is to use the crossplots to identify the relationship of log responses to rock type (Pickett 1977., Asquith 1979., Watney 1979).

Different models have been performed to get information about the rock type. On the basis of structure, different kind of the facies are identified which linked with petrophysical and lithological variation (Ahmad et al., 2002). Crossplots for the multiple log responses can be

used to establish relationship between logs response and rock type, provided some petrophysical data from cores and cutting is available (Asquith and Krygowski, 2004).

4.8.1 PHIE, GR and Depth Cross-plot

Figure 4.3 shows a cross-plot between effective porosity (PHIE), Gamma Ray log (GR) and depth of the formation under study. We can see the sand layer with good high effective porosity with low Gamma Ray log value at depth range of 3338 to 3346m. Three parts relative to the corresponding values are marked.

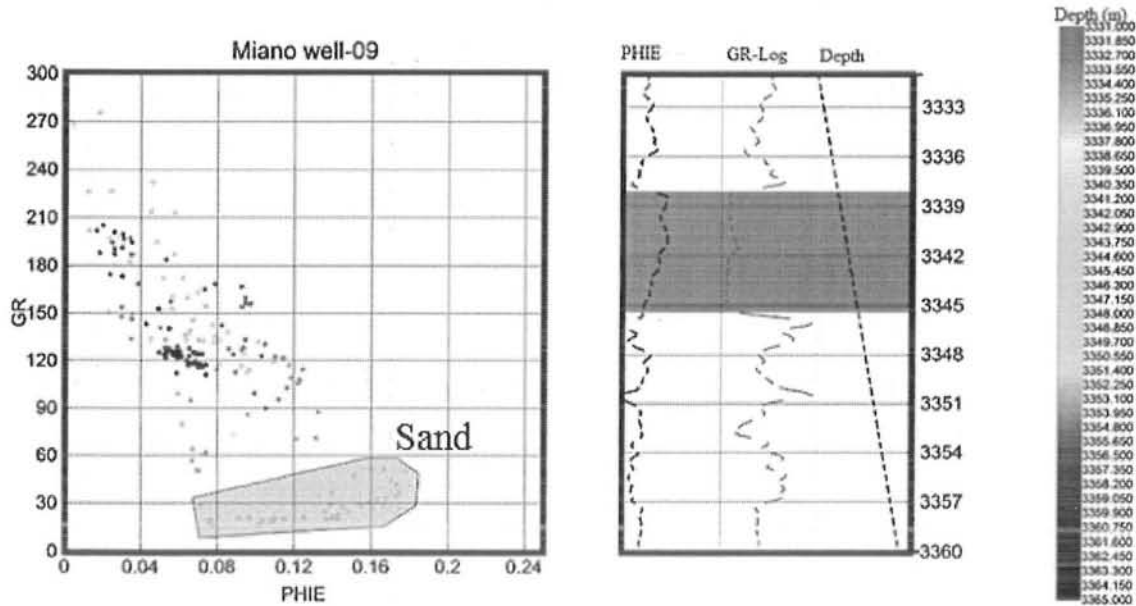


Figure 4.3: GR, PHIE & depth cross-plot.

4.8.2 NHPI, DT4P & GR Cross-plot

Figure 4.4 shows a cross-plot plotted between Neutron log (NPHI), density log (DT4P) and gamma ray log (GR). Low values of GR with high resistivity at depth range of 3338 to 3346m are observed. This is quite possibly the properties of sand layer with hydrocarbon.

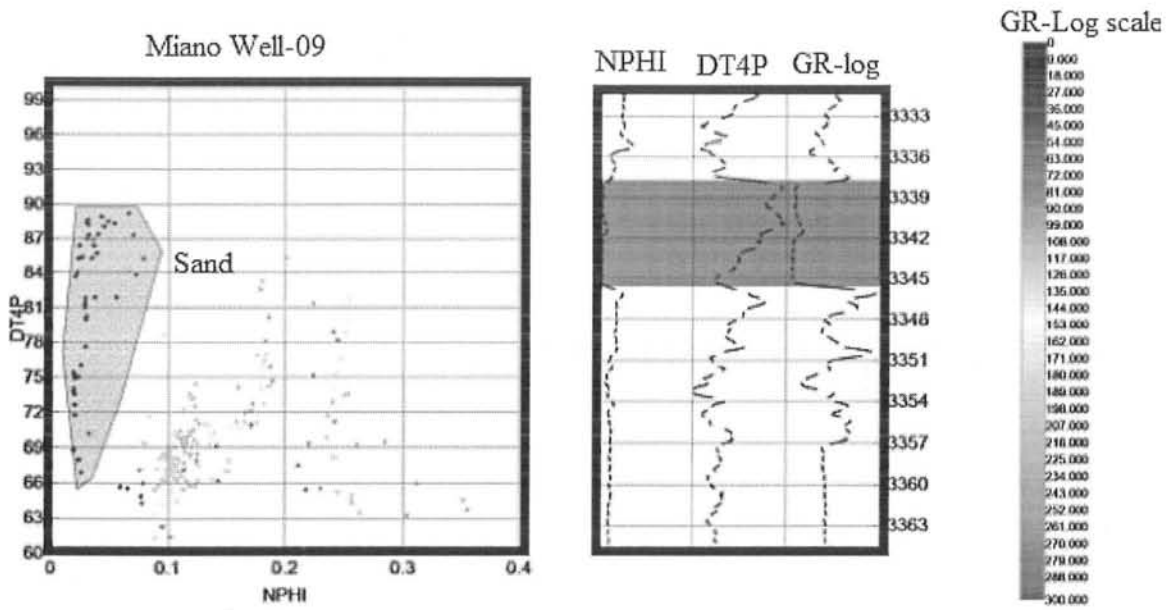


Figure 4.4: NPHI, DT4P & GR cross-plot.

4.8.3 NPHI, GR & Depth Cross-plot

Figure 4.5 shows a cross-plot plotted between gamma ray (GR), Neutron log (NPHI) and depth of the formation under study. A zone with low values of GR and even total porosity at depth range of 3338 to 3346 m marked is sand layer while greenish part reflects high GR and NPHI values satisfies shale presence. Sandy shale is often sandwiched in between sand and shale in the reservoir zone.

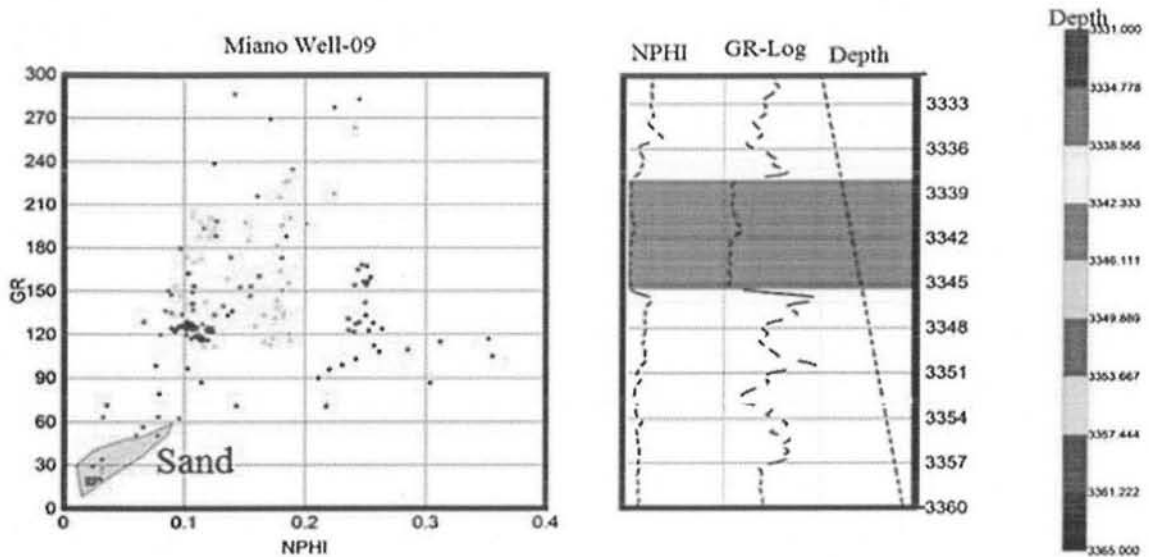


Figure 4.5: NPHI, GR & Depth Cross-plot.

Rock Physics:

5.1 Introduction

Through rock physics, the physical properties of the rocks in the real earth can be determined that varies vertically as well as laterally. According to Mavko (2009) regional averaged velocity function are used that shows the mean trend of the velocity with the depth. The RMS and the average velocities are not give the true representation of the earth subsurface so they cannot used for determined the rock properties. This provides an integrated methodology and practical tools for quantitative interpretation, characterization of reservoirs in the subsurface and assessment of uncertainty, using seismic and well-log data. RMS velocity is converted into interval velocities to compute several rock properties and generate graphs of P wave, S-wave, Density, Shear Modulus, Bulk Modulus, Young's Modulus, Poisson Ratio and Impedance for the subsurface layers to observe the behavior of these layers. The following formulas are used for computing Rock properties, for this purpose these formulas are inserted in the excel sheet to show the graphical representation of the above discussed rock properties (Mavko et al., 2009).

5.2 Rock Physics analysis

The term Rock Physics relates the geological properties (e.g. porosity, lithology, saturation) of a rock at certain physical conditions (e.g. pressure, temperature) with the corresponding elastic and seismic properties (e.g. elastic modulus, velocity, impedance).

1. Rock physics uses the sonic log, density log.
2. Rock physics establish the V_p , V_s and density and the relation between them.
3. Rock physics give the information about the rock property, impact of fluid and porosity on the V_p , V_s and poison ratio.
4. By observing the rock behavior of V_p , V_s , ratio of V_p versus V_s and the poison ratio we can described their behavior in the reservoir.
5. Rock Physics may use information provided by the Petrophysicist, such as shale volume, saturation levels, and porosity in establishing relations between rock properties or in performing fluid substitution analyses (Dewar 2001).

5.3 P-Wave (Primary Wave)

P-waves velocity has the most interest to seismology so called also the compressional wave, primary wave, longitudinal waves, and dilatation waves (see Fig. 3.12). During this wave the particle of the earth moves back and forth in the same direction and it will depend upon the density and elastic constants (Dobrin, 1976). The seismic velocity of a medium is a function of its elasticity and can be expressed in terms of its elastic constants.

For a homogeneous, isotropic medium, the seismic P-wave velocity V_p is given by

$$V_p = \sqrt{\left(\frac{4}{3}\mu + \kappa\right) \div \rho} \quad (5.1)$$

where,

- μ is the shear modulus.
- κ is the bulk modulus.
- ρ is the density of the medium.

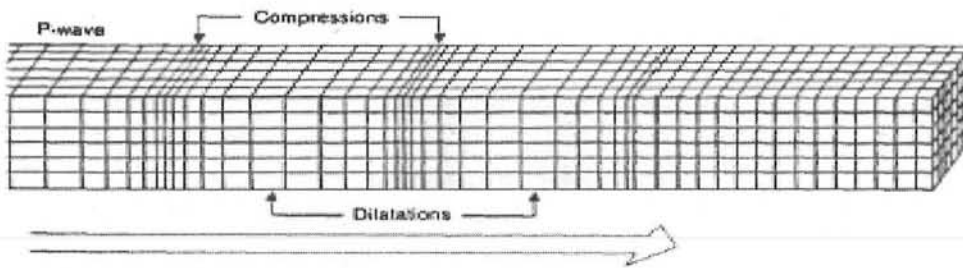


Figure 5.1: The propagation of P-waves in an Elastic Medium (Dobrin, 1976)

5.4 S-Wave (Secondary wave)

In shear waves, the particles vibrate in a direction perpendicular to the direction of propagation of waves (see Figure 5.2).

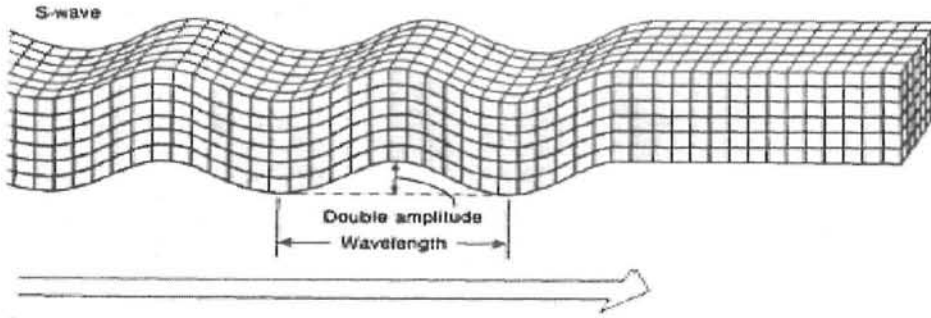


Figure 5.2: Propagation of S-waves in an Elastic Medium (Dobrin, 1976).

This will also called as Shear waves, transverse waves, and converted waves. In ideal cases for gases and liquid $\mu=0$. S-waves cannot pass through fluids, Dobrin (1976). The velocity of S-waves is given by;

$$V_s = \sqrt{\mu/\rho} \quad (5.2)$$

5.5 Poisson Ratio

Poisson's ratio is defined as the transverse strain divided by longitudinal strain. This means that it is the measure of incompressibility of the rock body. In post stack data shear wave velocity has been estimated only as a parameter because post stack data do not have shear components. Also Poisson's ratio is more dependent upon P-wave velocity rather than S-Wave velocity. Estimation of Poisson's ratio can be calculated by using formula

$$\sigma = \frac{1}{2} * \left(\left(\frac{V_p}{V_s} \right)^2 - 2 \right) / \left(\left(\frac{V_p}{V_s} \right)^2 - 1 \right) \quad (5.3)$$

where,

- σ =Poisson Ratio
- V_p = P-Wave velocity in m/sec
- V_s =Shear wave velocity is meter per second.

In other words we can say that the Poisson's Ratio is the measure of the behavior of a seismic wave when it passes through the rock body. Poisson ratio as above formula shows depends upon p-wave and s-wave and their variation with depth is discussed above in the chapter hence trending of Poisson ratio.

5.6 The V_p, V_s Ratio

It is found that compressional wave is sensitive to the saturating fluid type. So, the ratio of V_p and V_s is a good tool to understand a fluid type, G.M. Hamada (2004). The Figure 5.3 shows the fluctuation from 3338 to 3346 m , which is the reservoir zone.

5.7 Velocity Relation With depth:

Reservoir data set is obtain from the miano-09 well .We use the sonic log, to find the velocities V_s and V_p , Gr-log, Effective porosity is also calculated by using the sonic log and Neutron log and for the calculation of the saturation of water ,we use the LLD log and well borehole information.

In the first track of figure 5.3, there is the primary velocity (V_p) and in track two there is a V_s velocity. In track three, there is the V_p/V_s ratio and in track five, there is Poisson's ratio.

The main purpose of this calculation is to find out the behavior of velocity within depth in the reservoir and impact of the hydrocarbon on the velocity. From figure 1, it is shown that from 3338m to 3346m, V_p and V_s decreases and Poisson's ratio at that interval are decreases .Hence we can mark that there are hydrocarbon present there.

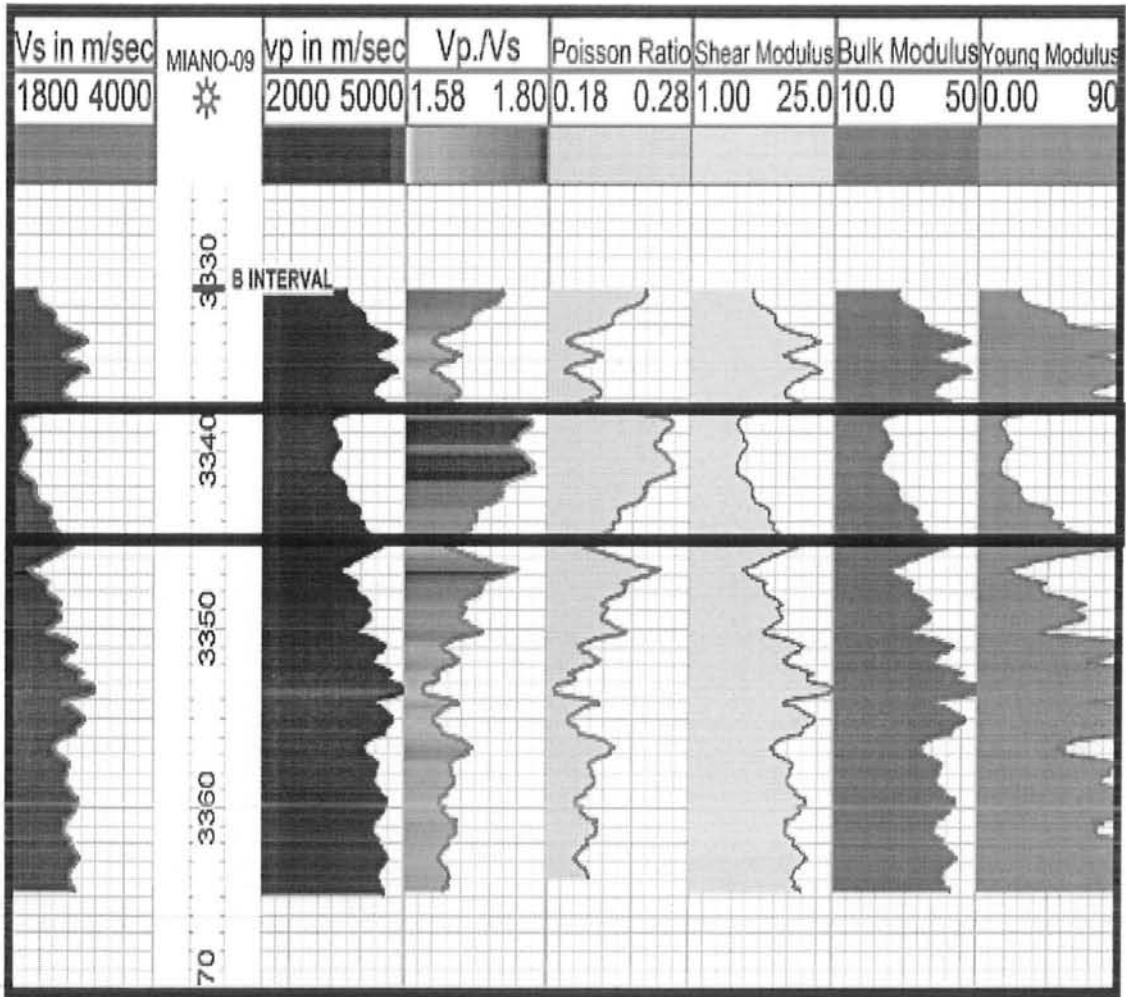


Figure 5.3: Velocity relations within depth

5.8 Young's Modulus (E)

In the solid mechanics, Young modulus (E) is the measure of the stiffness of an isotropic elastic material. It is also known as the modulus of elasticity. It is defined as, "the ratio of the uniaxial stress over the uniaxial strain in the range of stress in which Hook's Law holds" (Mavko et al., 2009).

The Young modulus can be calculated by using equation (1);

$$E = \sigma / \epsilon \quad (1)$$

where,

- E = young's modulus
- σ = Tensile stress

The Young modulus behavior, from depth 3331 to 3385m of well 09, shows that the stiffness of the subsurface strata shows the fluctuation (Figure 5.3).

Figure 5.4: Indicates Young's Modulus versus Depth

5.9 Bulk Modulus

The bulk modulus can be defined as the ratio of volume of stress to strain and it basically explain the substance's resistance to uniform pressure (Mavko et al., 2009).

For fluid only bulk modulus is meaningful. The bulk modulus is shown in Figure 5.3. This also shows the fluctuation in the bulk modulus curve with respect to depth of well 09 of miao area.

5.10 Shear Modulus

Shear modulus is defined as, “ the ratio of the shear stress to the shera strain”. This mostly concern with the deformation of a solid as it experices a force parallel to one of its surface while its opposite face experience an opposing force for fluid it is near above equal to zero.

$$\mu = \rho * V_s \quad (5.3)$$

where,

- μ = Shear modulus
- ρ = Density and V_s is S-wave velocity.

Shear Stress is shown in Figure 5.3. This figure shows the decrease in the Shear stress in the reservoir zone that is from 3338 to 3346 m.

SEQUENCE STRATIGRAPHY

6.1 An Overview

The most recent revolutionary paradigm is the sequence stratigraphy that is in the field of sedimentary geology. The concepts given by this way cause a fundamental change in the geological thinking and mostly in the facies and the stratigraphic analysis. Over the past fifteen years, stratigraphic approach has been introduced by geoscientists as the preferred style of stratigraphic analysis. This stratigraphic approach is encouraging the integration of data sets and the research method. The success and popularity of sequence stratigraphy popularity and success is because of its frequently used in the hydrocarbon exploration basins, (Octavian Catuneanu, 2006).

6.2 Sequence Stratigraphy

The cyclic sedimentation patterns analysis that they develop in response to change in the sediment supply. (Posamentier and Allen, 1999).

6.3 Sequence

The conformable succession related to the strata that are bounded by the unconformable succession. (Mitchum, 1977).

6.4 Sequence stratigraphy and Sea Level Change

- (a) Transgression will occur at the time when the sea level raises abruptly then that of the sediment supply and the pattern in the sediments is retrogradational.

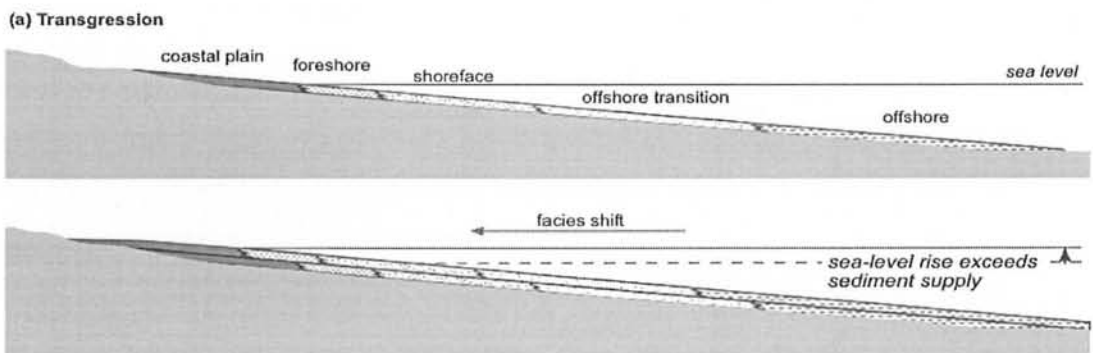


Figure 5.1: Transgression (Nichols, 2009)

- (b) Regression phenomenon will occur when sediment is supplied to a coast where there is no (or relatively slow) sea-level rise the coastline moves seaward: this is and the sediment pattern is progradational.

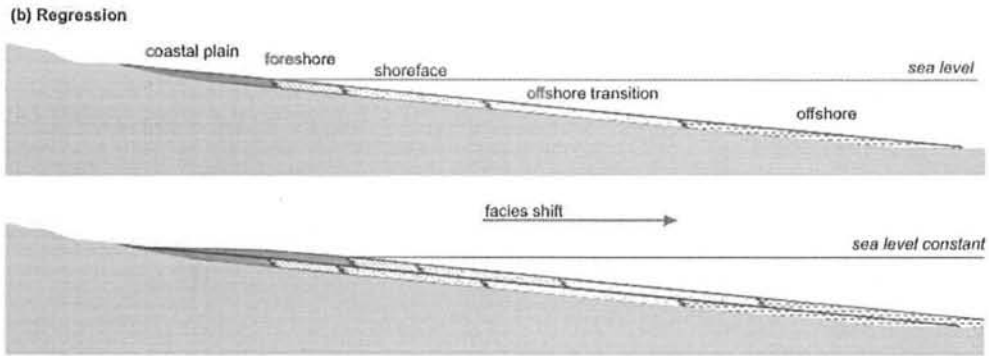


Figure 5.2: Regression (Nichols, 2009)

(c) Forced regression is the result of the Sea-level fall and the sediment pattern is retrogradational, and may include erosion surfaces.

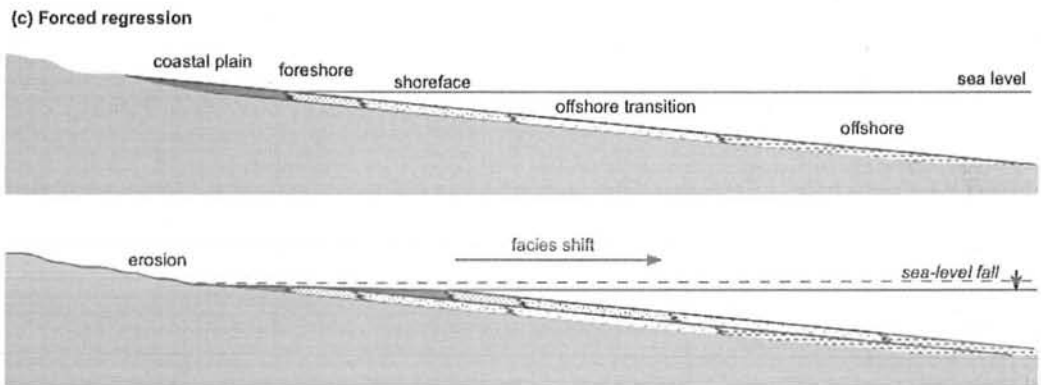


Figure 5.3: Regression (Nichols, 2009).

(d) A situation where there is the balance between the sediments supply and the sea level rise or fall then this phenomenon is known to be aggradation. This will be occur in two condition either the sea level rise or fall but the total supply of the sediments will remain same as that of the sea level fluctuation.

(e)

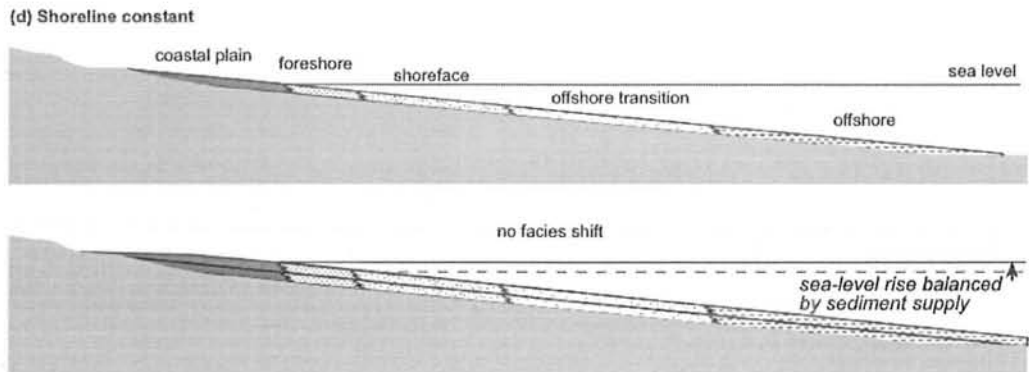


Figure 5.4: Aggradation (Nichols, 2009)

6.5 Depositional Environment Related to Well Log

Depositional environment play important rule in the hydrocarbon exploration. Mostly well will dry because of not enough information about the depositional environment of the sediments as sediments deposition changed. We use Miano well-09 to interpret the deposition of the sediment. We use the GR-log for this purpose and interpret the B-Interval and C-interval.

6.6 C-Interval

The top of the C-Interval is 3167m. From 3230m to 3240m log curve shown that at that depth retrogradational phenomenon will occur and as we move towards the top of the C-Interval log cure will show the progradational phenomenon and from this will shows that sediment (sand) will show the coarsening upward. GR-log of the C-interval is shown in the Figure 5.6.

6.7 B-Interval

The top of the B-Interval is 3331m. The log curve of GR-log will show that at this interval progradational phenomenon is observed as shown in the Figure 5.7. GR- log curve shows the channel fill and from 3338 to 3346 m shows the flat and this is a pay zone.

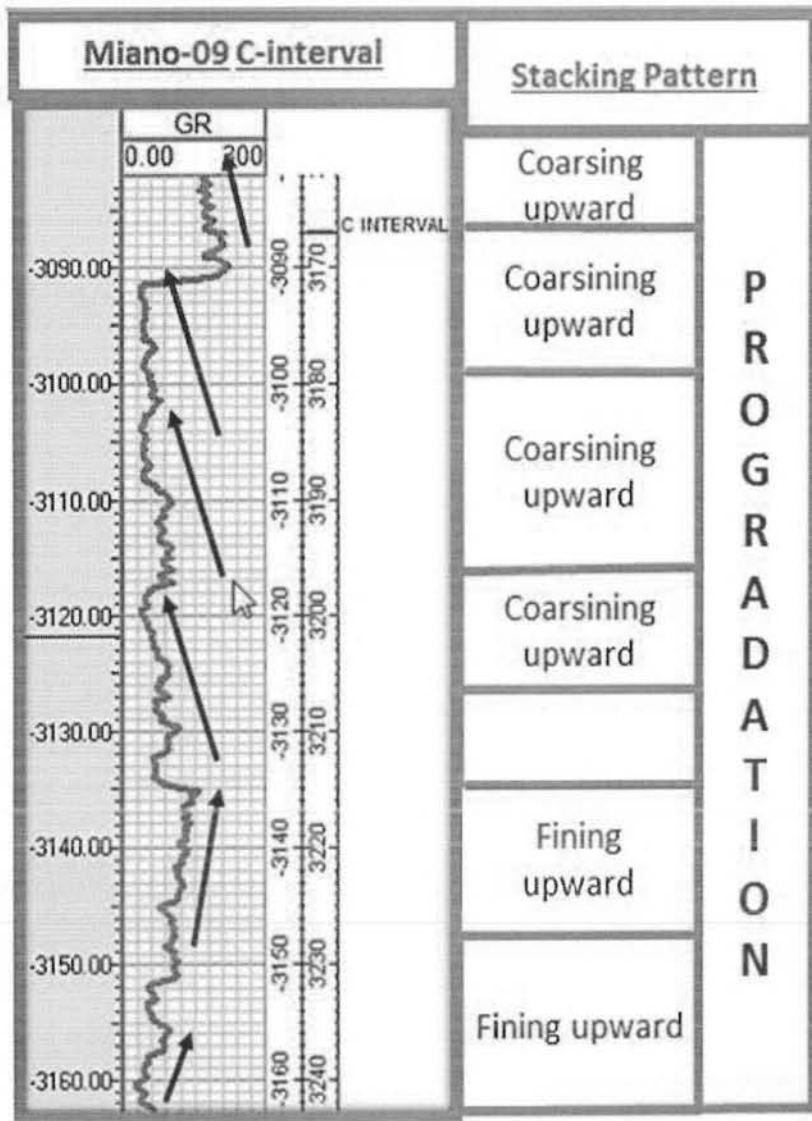


Figure 5.5: Depositional Environment of C-Interval

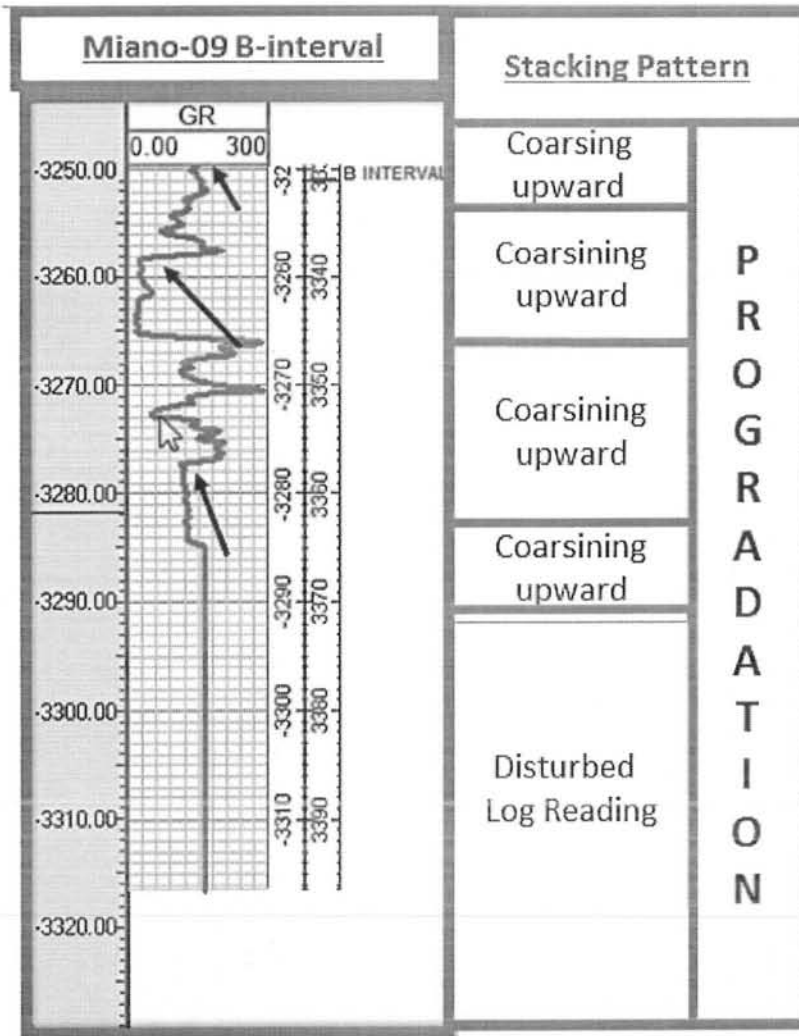


Figure 5.6: Depositional environment of B-interval

Amplitude versus Offset

7.1 Introduction

Seismic interpretation are the process, through which we are able to obtain information, having experiences about the geology and geophysics, where as in the qualitative interpretation one has to apply approximation sand techniques for estimation of zone of interest. AVO analysis is the technique that is used by geoscientist to evaluate reservoir's porosity, density, velocity, lithology and fluid content. Variation in seismic amplitude is associated with change in lithology and fluid content in the rock above and below the reflector as the distance between source and receiver is changed. Because of complexity of the earth's subsurface, different rocks have different response to AVO although these rocks are filled with same fluid and have same porosity (Almutlaq and Margrave, 2010).

The change in the transmission coefficient and reflection coefficient with the angle of incidence (AVA) is also known to be the offset reflectivity and this is the basic basis for AVO analysis, (Hongbo Zhang and R. James Brown, 2001).

7.2 Amplitude Versus offset (AVO) Analysis

Ostrander (1984), 12 years after the bright spot technology became a commercial tool for hydrocarbon exploration, published a break through paper in Geophysics. Then, year after, Shuey (1985) confirmed mathematically via approximations to Zoeppritz exact solutions that Poisson's ratio most directly related to offset dependent reflectivity for incident angles up to 40° . AVO technology, a commercial tool for oil industry, was born. Schematic flow for process of AVO analysis is shown in following figure (7.1).

Amplitude versus offset or AVO is the change of the amplitude within the CDP gather.

The rate of change in amplitude seems to be related to the porosity of the rock and the near impedance reflects the fluid changes while shear wave velocity remains roughly the same. With non-normal angle of incident we create shear wave in the data. This change in time V_p/V_s creates the AVO or the anomalous behavior of amplitude with angle. V_p/V_s are the proportional to Poisson ratio so when we see change in the V_p/V_s then we see change in the Poisson ratio.

As discussed above Acoustic impedance or AI is one of the main drivers of AVO. When we describe a class of AVO we define it by the acoustic impedance between the encasing shales and reservoir sand (Resnick et al, 1987).

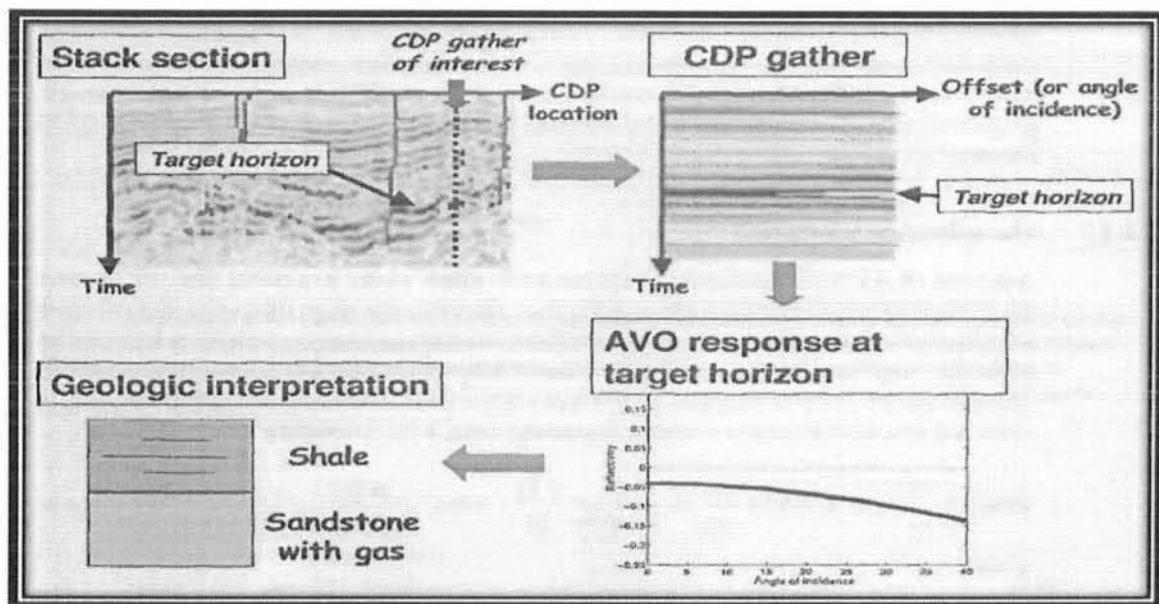


Figure 7.1: Schematic procedure for AVO analysis

AVO analysis is based on the Knott and Zoeppritz equations (Knott, 1899, and Zoeppritz, 1919). This will describe the various reflection and transmission coefficients for plane waves (Treitel and Lines, 1988).

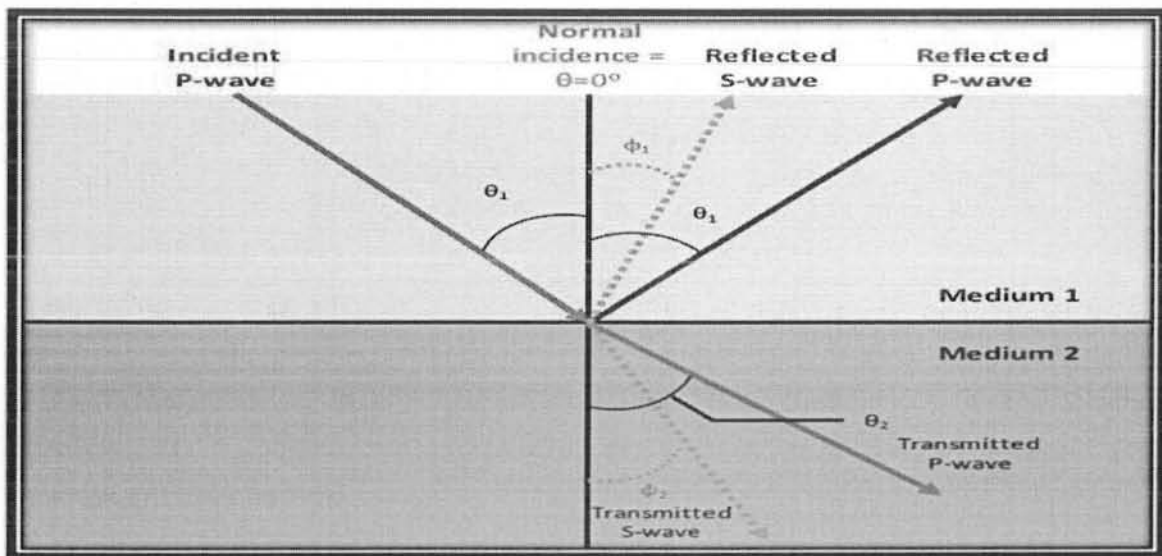


Figure 7.2: For an incident P-wave the Reflection and Transmission at an interface (Almutlaq & Margrave, 2010).

7.3 Zoeppritz equation

This equation narrates the amplitude of the transmitted and the reflected P-wave and S-wave. When wave i-e P-wave incident at the boundary between two elastic media. In such a way two reflected and two transmitted waves are generated as a result. The energy of that component depends upon the P-wave and S-wave velocities, the angle of incidence and density. Figure (7.2) describes the reflection, transmission, and mode conversion of a P-wave at a two elastic media.

7.4 Shuey's Approximation (1985)

Shuey (1985) tried to make the equation into the linear equation $y = mx + c$ where m is the gradient and b is the intercept, here we get the concept of the terms intercept and gradient. If we were to plot amplitude versus square of $\sin \theta$ where θ is the angle of a single seismic event then the incident would be zero offset stacked and the gradient is the slope of the best-fit line. Change in the gradient could reflect in the changed in lithology but it also reflect the change in the fluid. This approximation is good to about 30° of incidence angle. Shuey's approximation is given as equation (1)

$$R_\theta = A + B \sin^2 \theta + C \sin^2(\theta) \tan^2(\theta) \tag{1}$$

$$\text{Intercept} = \frac{1}{2} \frac{\Delta(\rho\alpha)}{\rho\alpha} \quad \text{Gradient} = \frac{1}{2} \frac{\Delta(\alpha)}{(\alpha)} - \frac{4\beta^2}{\alpha^2} \frac{\Delta\beta}{\beta} - 2 \frac{\beta^2}{\alpha^2} \frac{\Delta\rho}{\rho} \quad \text{Curvature} = \frac{1}{2} \frac{\Delta\rho}{\rho}$$

Acoustic Impedance

V_p/V_s

V_p

0-15

15-30

30-35

Intercept-Curvature

$$\frac{1}{2} \frac{\Delta\rho}{\rho} + \frac{1}{2} \frac{\Delta\alpha}{\alpha} - \frac{1}{2} \frac{\Delta\alpha}{\alpha} \rightsquigarrow \frac{1}{2} \frac{\Delta\rho}{\rho}$$

0-15 30-45

7.5 Rouger Approximation

AVO analysis is done to find out information about the physical properties from the earth compressional wavefield. Shuey equation can't easily interpret the gradient in term of shear wave velocity of upper and lower media. Hence, in such a case Rouger approximation is used that is given in equation (2)

$$R_p^{iso} i = \frac{1}{2} \frac{\Delta Z}{Z} + \frac{1}{2} \frac{\Delta V_p}{V_p} - \frac{2 V_p}{\Delta V_p} \frac{\Delta G}{G} \sin^2 i + \frac{1}{2} \frac{\Delta V_p}{V_p} \sin^2 i \tan^2 i \quad (2)$$

7.6 AVO Classification:

AVO classification had been described by the Rutherford and Williams to characterize for the seismic reflection from the interface between sand and shale in 1989. This classification has become as an industrial standard for the gas sands. They explain four types of classes.

Class 1: Gas-Sandstone with Higher impedance

In Class 1, sandstone has higher impedance than its cover (shale). The high reflection coefficient and the positive zero offset will be generated because of the shale sand interface. Gradient of Class 1 sandstone has greater than class 2 and class 3.

Class 2: Near zero impedance contrast gas sandstone

Sandstone of class 2 at the interface has equal contrast of acoustic impedance with amplitude that is increasing with offset. This type of sand class has the negative reflection coefficient at zero offset.

Class 3: Low impedance Gas sandstone with low impedance

Class 3 has lower acoustic impedance than its cover.

Class 4:

At zero offset, Class 4 has negative reflection coefficient and lower impedance with amplitude that is decreasing against the offset. At a certain angle, there is a change in polarity and then amplitude will increase proportionally to the offset.

The class of sand shown in the Figure 7.1

Table 7.1 Behavior of the Various Gas Sand Classes

Sand Class	Relative Impedance	Amplitude Vs. offset
I	greater than that of overlying unit	Decreases
II	same as the overlying unit	This may change sign Increase or decrease:
III	Lesser than overlying unit	Increases
IV	Lesser than overlying unit	Decreases

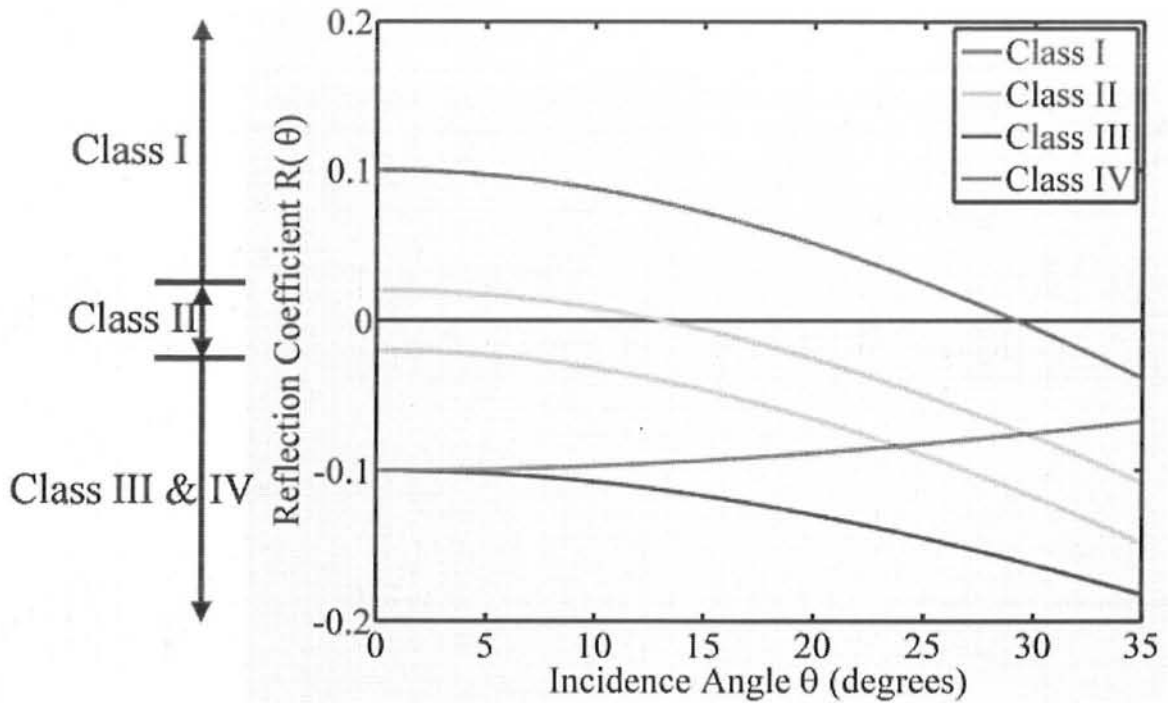


Figure 7.3: AVO classification (Oil and Natural Gas Corporation)

7.7 AVO Modling in the Study area

Data set has been obtained from the Miano area, from miano-09 well. Sonic log of miano-09 well is used to calculate the V_p , V_s and density of the C-interval and the B-interval as mentioned in above that C-interval is the cape rock and the B-interval is the reservoir rock. To find the class of sand we use the exact equation, the Rouger approximation and Shuey approximation. It is shown in the figure 7.4 that Rouger approximation is best related to exact while the Shuey approximation is not. This will show the limitation of Shuey approximation in our area. This figure 7.3 describes the characteristics of class 1 sand.

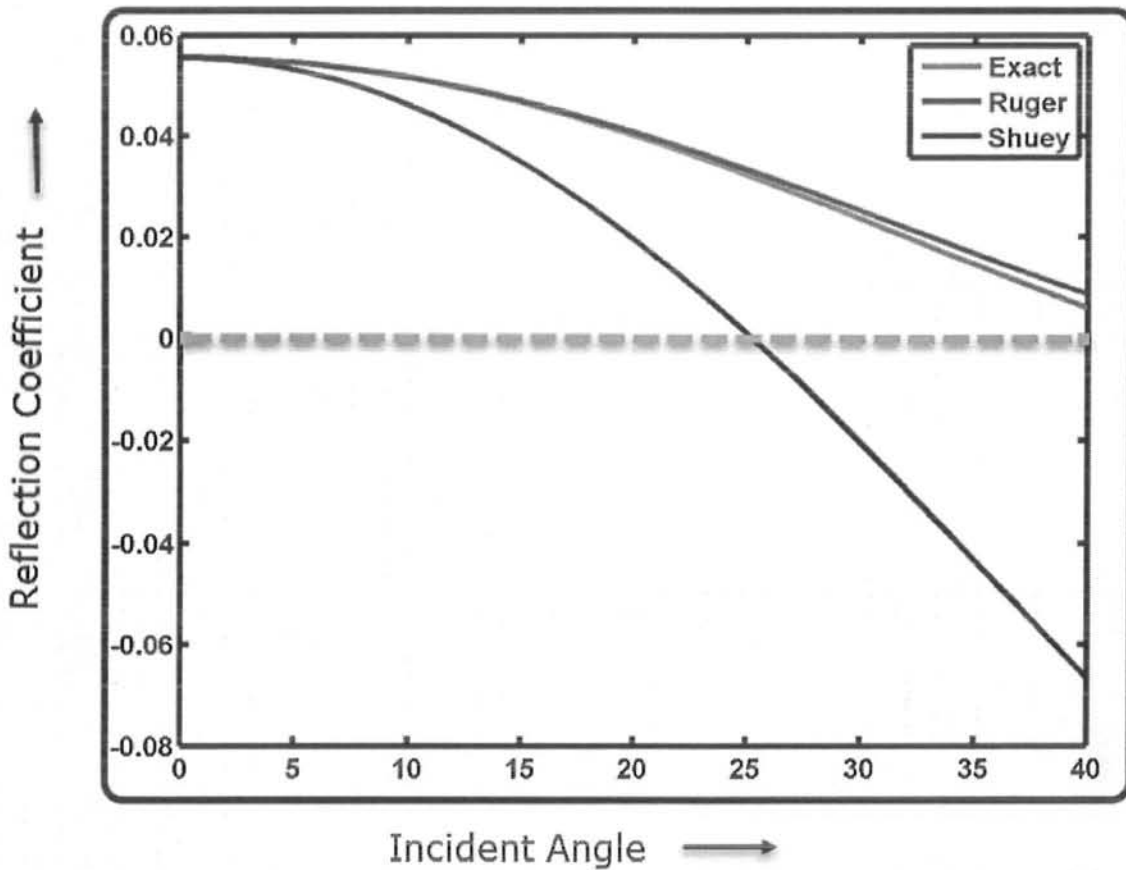


Figure 7.4 AVO Classification in the Miano area

7.8 Wavelet Analysis

The term wavelet is used to explain a short time series that is used to show the source function. Wavelet can be studied as a time domain or in the frequency domain. Time domain wavelets are in any amplitude spectrum which can be constructed by varying the phase spectrum. (Wickerhauser, 1994).

7.8.1 Deconvolution

Reverse process of the convolution process is known to be the Deconvolution. Convolution in the time domain is that represented in the frequency domain by a multiplying the amplitude spectra and adding the phase spectra. In principal by deconvolving the source wavelet we could obtain the earth's reflectivity, (Wickerhauser, 1994). The spikes are closer together is shown in figure 7.5. If the information is given about the wavelet then input spike series can be discovered by the deconvolution process.

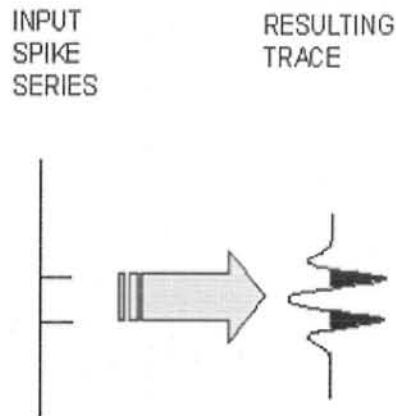
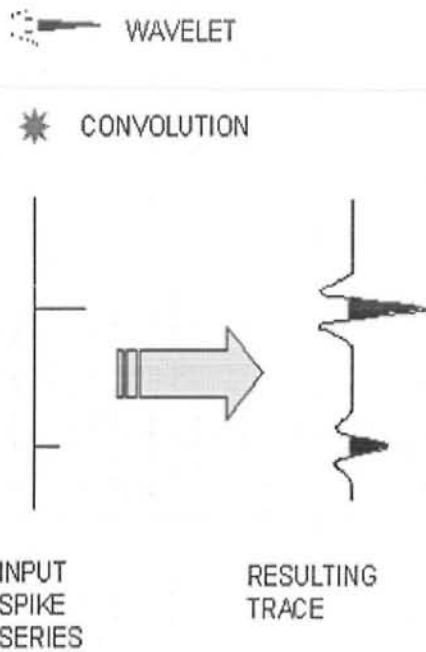


Figure 7.5: Deconvolution (Wickerhauser,1994).

7.8.2 Convolution

In convolution method two signals are combining by the mathematical way to achieve third, modified signal. Wavelet at the spike times and with the spike amplitudes is shown in figure in the figure (a). The convolution process just involves multiplying every sample of the spike series by the input wavelet and adding all the results. (Wickerhauser,1994).



7.6 Ricker Wavelet (Wickerhauser,1994).

A Ricker wavelet is often used for the modelling purpose which is defined by its dominant frequency. The Ricker wavelet is by definition zero-phase, but a minimum phase equivalent can be constructed. It is simple to understand and often seems to represent a typical earth response. The Ricker wavelet at frequency 40 Hz which denoted by $w(t)$ and time interval 0.002s is shown below. The Figure 7.7 shows that at time 33 to 43s, there is peak in the frequency.

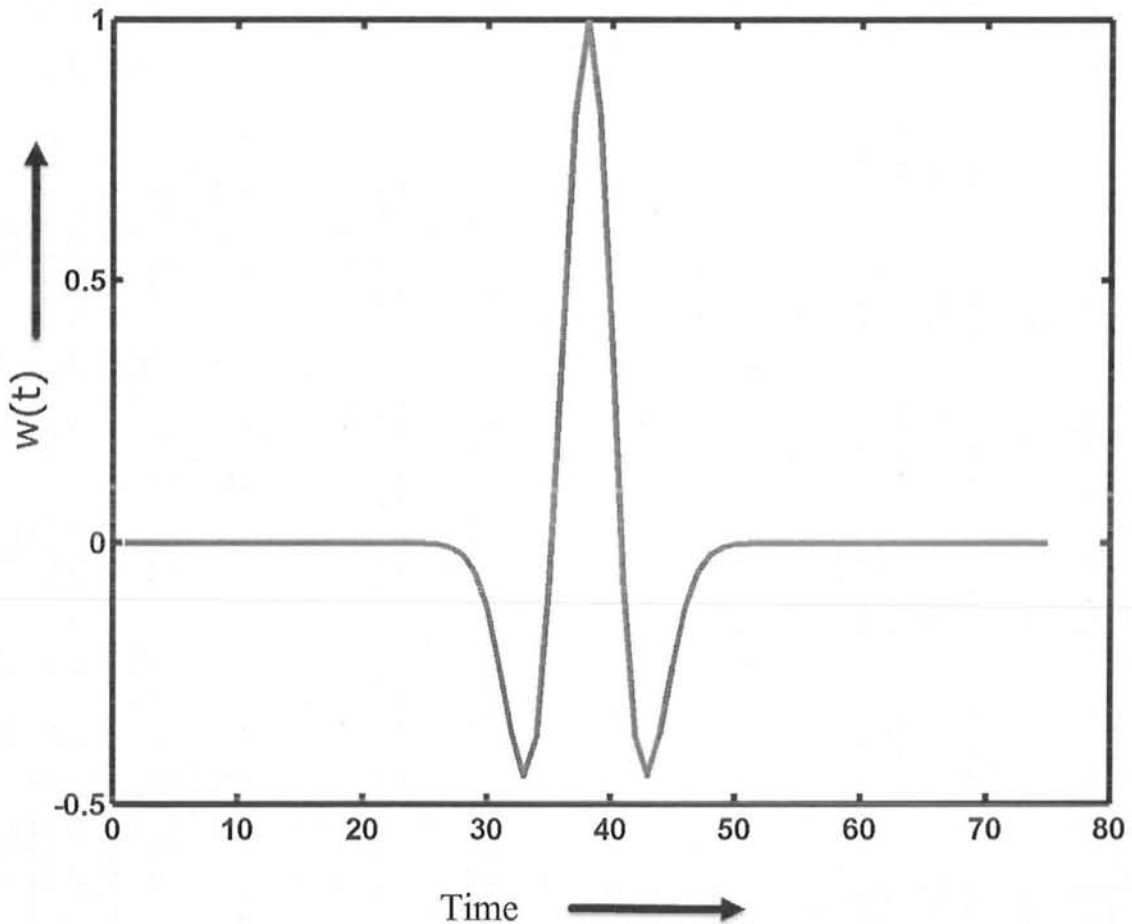


Figure 7.7 Ricker Wavelet

7.9 Convolution Ricker Wavelet with Exact, Rouger and Shuey:

Data has been obtained from the miano-09 well. Here we convolve the Ricker wavelet with exact, Shuey and Rouger. Exact wavelet after the convolution with the Ricker wavelet is express in red color. Similarly Ruger wavelet in green color and Shuey wavelet is in the purple color. These will be shown in figure 7.8.

The main purpose of this to describes the polarity change with frequency. From the figure 7.8 shows that the Exact and Rouger wavelet has same result throughout the result but in case of the Shuey it the reverse case. From this figure we can conclude the result that Shuey approximation has some limitation to our area while Rouger gives some fruitful results.

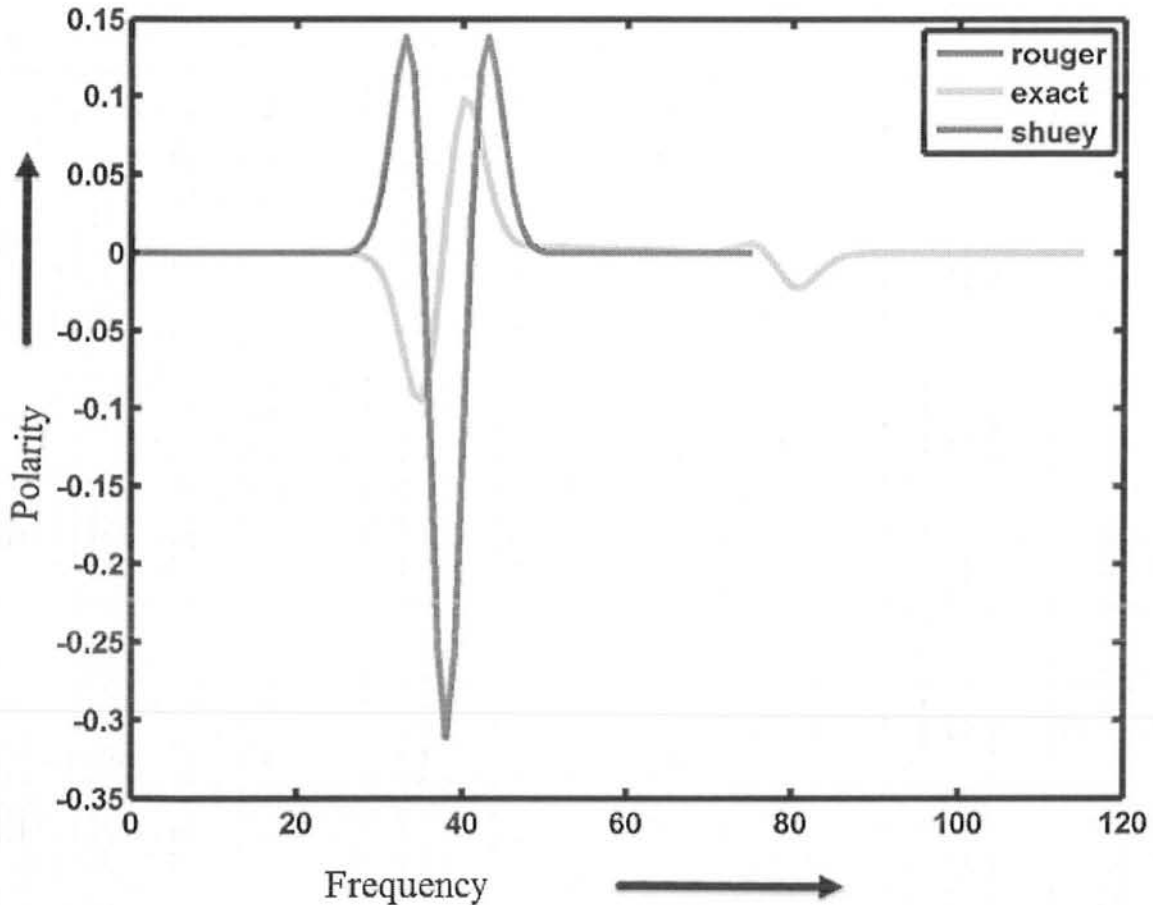


Figure 7.8 Convolution of Ricker Wavelet with Shuey, Rouger and Exact

7.10 Velocity and Lithology

Sonic logging and the seismic has the important role. For the understanding of these and other geophysical technique, some have to understand the acoustic property of the rock. Acoustic velocities V_p and V_s can be express simply in term of elastic constant and the density of the medium. The elastic constants and the density depend upon the porosity, fluid property, pressure and temperature of the subsurface lithology (Guéguen et al., 1994).

In case of the sedimentary rock, each rock has impact on the V_p . In case of sand and shale V_p (km/sec) has the range 2 to 5.5(km/sec) and 1.8 to 4.0 (km/sec) respectively. Lithology

can be marked on the bases of velocities (Guéguen et al., 1994). Figure 7.8 describes the V_p/V_s as a function of Poisson ratio (ν). Poisson ratio (ν) is described in the above chapter. The lithology's are marked as shown in the figure 7.9

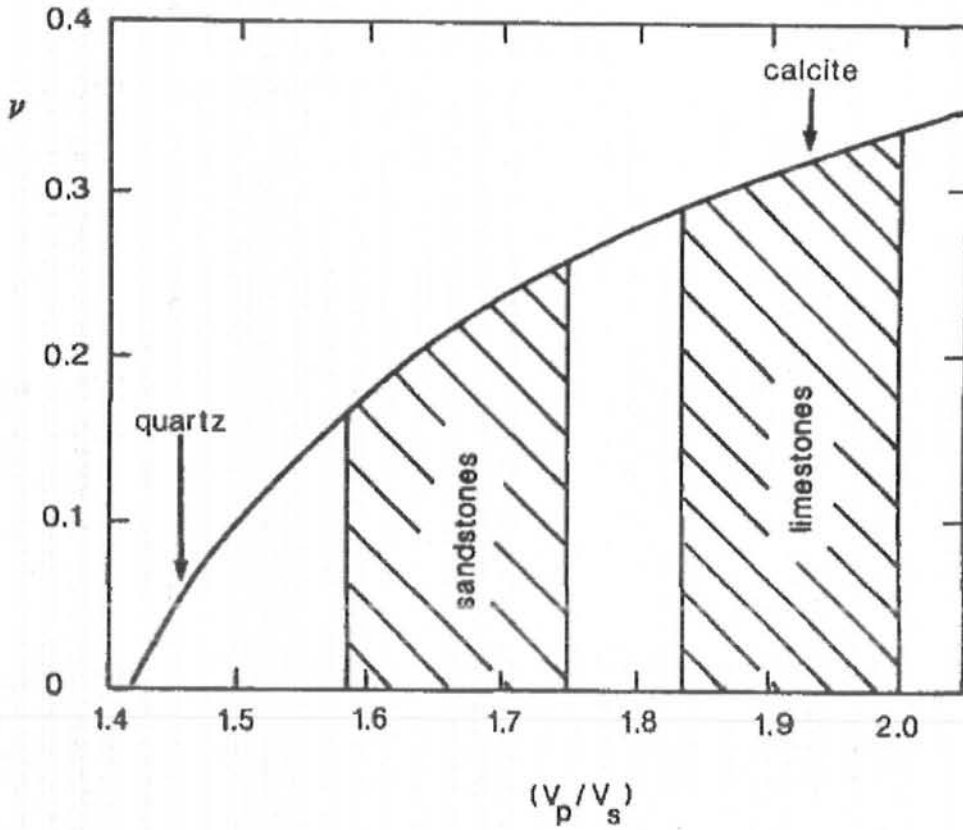


Figure 7.9 V_p/V_s ratio as a function of Poisson ratio (Guéguen et al, 1994)

7.10.1 Lithology Identification in the Reservoir (B-interval)

In Miano area, B-interval (Lower Goru) is the reservoir. Here data is used miano-09 well. Here V_p , V_s and Poisson ratio is calculated by using the sonic log. Sandstone Lithology is marked in the figure 7.10 on the basis of figure 7.9.

Chapter 03

1. Bakker, P. (2002). Image structure analysis for seismic interpretation. *Delft University of Technology*.
2. Leever, K. A., Matenco, L., Bertotti, G., Cloetingh, S. A. P. L., & Drijkoningen, G. G. (2006). Late orogenic vertical movements in the Carpathian Bend Zone—seismic constraints on the transition zone from orogen to foredeep. *Basin Research*, 18(4), 521-545.
3. McQuillin, R., Bacon, M., & Barclay, W. (1984). An introduction to seismic interpretation-Reflection seismics in petroleum exploration.
4. Coffeen, J. A. (1986). Seismic exploration fundamentals.

Chapter 04:

1. Asquith, G. B., Krygowski, D., & Gibson, C. R. (2004). *Basic well log analysis* (Vol. 16). Tulsa, OK: American association of petroleum geologists.
2. Croizé, D., Ehrenberg, S. N., Bjørlykke, K., Renard, F., & Jahren, J. (2010). Petrophysical properties of bioclastic platform carbonates: implications for porosity controls during burial. *Marine and Petroleum Geology*, 27(8), 1765-1774.
3. de Jong, M. G. G., Nio, S. D., Biewinga, D. T., & Smith, D. G. (2004, September). Advances in the Interpretation of Geophysical Borehole Logs. In *Near Surface 2004-10th EAGE European Meeting of Environmental and Engineering Geophysics*.
4. Hamada, G. M. (2004). Reservoir fluids identification using Vp/Vs ratio?. *Oil & Gas Science and Technology*, 59(6), 649-654.

Chapter 05

1. Mavko, G., Mukerji, T., & Dvorkin, J. (2009). *The rock physics handbook: Tools for seismic analysis of porous media*. Cambridge university press.